Reversion-inducing cysteine-rich protein with Kazal motifs interferes with epidermal growth factor receptor signaling

著者	Kitajima Shunsuke, Miki T., Takegami Yujiro, Kido Y., Noda M., Hara Eiji, Shamma Awad, Takahashi Chiaki
journal or publication title	Oncogene
volume	30
number	6
page range	737-750
year	2011-02-10
URL	http://hdl.handle.net/2297/27079

doi: 10.1038/onc.2010.448

ORIGINAL ARTICLE ONC-2010-00260-R

Reversion-inducing cysteine-rich protein with Kazal motifs (RECK) interferes with epidermal growth factor receptor (EGFR) signaling

Running title: RECK antagonizes RAS signaling

S Kitajima[1,2], T Miki[2,3,4], Y Takegami[2], Y Kido[1], M Noda[2], E Hara[5], A Shamma[1,2,3] and C Takahashi[1,2,3]

[1]*Division of Oncology and Molecular Biology, Cancer and Stem Cell Research Program, Cancer Research Institute, Kanazawa University, Kakuma-machi, Kanazawa, Ishikawa 920-1192, Japan*

[2] *Department of Molecular Oncology, Kyoto University Graduate School of Medicine, Yoshida-Konoe-cho, Sakyo-ku, Kyoto 606-8501, Japan*

[3] *The 21st Century Center of Excellence Program, Kyoto University Graduate School of Medicine, Yoshida-Konoe-cho, Sakyo-ku, Kyoto 606-8501, Japan*

[4] *Department of Biochemistry and Molecular Biology, University of Texas Health Science Center-Houston, Houston, Texas 77030, USA*

[5] *Division of Cancer Biology, The Cancer Institute, Japanese Foundation for Cancer Research, 3-8-31 Ariake, Koto-ku, Tokyo 135-8550, Japan*

Correspondence: Professor C Takahashi, Division of Oncology and Molecular Biology, Cancer and Stem Cell Research Program, Cancer Research Institute, Kanazawa University, Kakuma-machi, Kanazawa, Ishikawa 920-1192, Japan.
E-mail: chtakaha@staff.kanazawa-u.ac.jp

Abstract

The *reversion-inducing cysteine-rich protein with Kazal motifs* (*RECK*) gene had been isolated as an antagonist to RAS signaling; however the mechanism of its action is not clear. In this study, the effect of loss of RECK function was assessed in various ways

and cell systems. Successive cell cultivation of MEFs according to 3T3 protocol revealed that the germ-line knockout of *Reck* confers accelerated cell proliferation and early escape from cellular senescence associated with downregulation of $p19^{Arf}$, Trp53 and $p21^{Cdkn1a}$. In contrast, shRNA-mediated depletion of RECK induced irreversible growth arrest along with several features of the *Arf*, *Trp53* and *Cdkn1a*-dependent cellular senescence. Within two days of RECK depletion, we observed a transient increase in AKT and ERK phosphorylation associated with an upregulated expression of cyclin D1, $p19^{Arf}$, Trp53, $p21^{Cdkn1a}$ and Sprouty 2. On further cultivation, RAS, AKT and ERK activities were then downregulated to a level lower than control, indicating that RECK depletion leads to a negative feedback to RAS signaling and subsequent cellular senescence. In addition, we observed that EGFR activity was transiently upregulated by RECK depletion in MEFs, and continuously downregulated by RECK overexpression in colon cancer cells. These findings indicate that RECK is a novel modulator of EGFR signaling.

Keywords: senescence; negative feedback; *RECK*; *EGFR*; *AKT*; *ERK*; *RAS*; *MMP*

Introduction

The *reversion-inducing cysteine-rich protein with Kazal motifs* (*RECK*) gene is a negative transcriptional target of various viral oncogenes including activated K-*ras* (Takahashi *et al.*, 1998; Sasahara *et al.*, 1999; Hsu *et al.*, 2006; Liu *et al.*, 2003), and a negative post-transcriptional target of oncogenic microRNAs including miR-21 (Hu *et al.*, 2008; Gabriely *et al.*, 2008; Zhang *et al.*, 2008; reviewed in Nicoloso *et al.*, 2009; Loayza-Puch *et al*., 2010). Furthermore, histone modification and DNA methylation have also been reported to be involved in the transcriptional regulation of *RECK* (Chang *et al.*, 2004; Chang *et al.*, 2006; Chang *et al.*, 2007). RECK expression is frequently correlated with a favorable prognosis in patients with various types of cancer (reviewed in Clark *et al*, 2007; Noda and Takahashi, 2007). However, the biological significance of these findings and mechanisms underlying them are still unclear. RECK has been proposed to be implicated in the extracellular signaling (Morioka *et al.*, 2009), but it is not clear which signaling pathway (receptor) is actually influenced by RECK. Although

our previous reports indicated that RECK exerts its functions through interaction with matrix metalloproteinases (MMPs) and a disintegrin and metallopeptidase 10 (ADAM10) (Takahashi *et al.*, 1998; Oh *et al.*, 2001; Miki *et al.*, 2007; Muraguchi *et al.*, 2007), it is still difficult to determine whether RECK is a *bona fide* membrane-anchored MMP/ADAM inhibitor, or whether MMP/ADAM inhibition is one of its multiple functions. We recently identified two RECK domains whose primary structures are homologous to that of a common substrate of several MMPs, and these domains were very slowly cleaved by the excessive amount of MMPs (Takegami and Takahashi, in preparation for publication). This may explain the ability of recombinant soluble RECK to competitively inhibit the proteolytic activity of recombinant soluble MMPs or membrane type 1-matrix metalloproteinase (MT1-MMP), even though its inhibitory effect on these protease activities is weaker than tissue inhibitors of metalloproteinases (TIMPs) in *in vitro* assays (Takahashi *et al.*, 1998; Oh *et al.*, 2001; Miki *et al.*, 2007; Omura *et al.*, 2009).

RECK modulates the endocytic pathways of membrane-tethered metallo-endopeptidases such as MT1-MMP and CD13/aminopeptidase N (APN) by changing their abundance in lipid raft through direct interaction (Miki *et al.*, 2007). This appeared to shorten the life span of these membrane-tethered enzymes. *Reck*-deficient mouse embryos show premature differentiation in cortical neurons due to downregulated Notch signaling caused by aberrant shedding of Delta-Serrate-Lag2 (DSL) ligands in an ADAM10-dependent manner (Muraguchi *et al.*, 2007 and reviewed in D'Souza *et al.*, 2008; Zolkiewska, 2008). RECK appeared to bind directly to ADAM10 and allosterically inhibit its proteolytic activity (Muraguchi *et al.*, 2007). In contrast, the recombinant RECK protein has been shown to competitively inhibit MMPs (Takahashi *et al.*, 1998; Oh *et al.*, 2001; Miki *et al.*, 2007; Omura *et al.*, 2009). RECK and Delta-like family proteins (D'Souza *et al.*, 2008; Zolkiewska, 2008) share structurally similar epidermal growth factor (EGF)-like repeats which may serve as recognition signals for ADAM10. Although identification of the domains responsible for such protein-protein interaction is currently hampered by the extremely cysteine-rich primary structure of RECK (Takahashi *et al.*, 1998), these findings suggest that RECK may function as more than a protease inhibitor.

To further address the basic functions of RECK in cells, in this study, we at first compared the short- and long-term effects of germ-line knockout to those of shRNA-mediated knockdown of RECK in early passage mouse embryonic fibroblasts (MEFs). By shedding light on the differential effects of RECK-deficiency dependent on the timing of downregulation, we attempted to identify cell signaling pathways modulated by RECK. Previous studies have linked RECK-deficiency to deregulation of extracellular gelatinase activities and focal adhesion stability (Oh *et al.*, 2001; Morioka *et al.*, 2009); however, these studies employed *Reck*-deficient MEFs that have been cultivated for a long time (more than 35 passages). In this study, we propose that the primary effect of RECK-deficiency appears in the control of cell cycle and cellular senescence. We identified EGFR/Ras pathway as one of the signaling pathways that are controlled by RECK.

Results

Differential effects of germ-line knockout and shRNA-mediated knockdown of RECK on cell proliferation

Consistent with a previous report (Hatta *et al.*, 2009), RECK expression was induced in MEFs by serum starvation, and downregulated after release from serum restriction (Figure S1a). Moreover, contact inhibition-dependent cell cycle arrest in the presence of serum was correlated with the increased RECK expression (Figure S1b). These findings implicated involvement of RECK in cell cycle control. In low passage number cell cultures, *Reck*$^{-/-}$ MEFs did not show remarkable differences in growth properties and gelatinase activities when compared to wild type or *Reck*$^{+/-}$ littermates (data not shown). However, successive cell cultivation of primary embryonic fibroblasts prepared from live embryonic day (E)10.0 embryos according to 3T3 protocol (Todaro and Green, 1963) revealed that after around 10 passages, *Reck*$^{-/-}$ MEFs displayed a higher proliferation rate, immortal cell growth and smaller cell size in comparison to wild type littermates (Figure 1a and data not shown); these findings suggest that germ-line knockout of *Reck* confers accelerated cell proliferation and early escape from cellular senescence. These phenotypes were correlated with downregulation of p19^{Arf}, Trp53 and p21^{Cdkn1a} (Figure 1b), and suppressed by the forced expression of p21^{Cdkn1a} (Figure 1c).

We then attempted to determine the function of RECK in cells by directly depleting RECK in wild type MEFs. Opposing to the results of the long-term analysis of germ-line knockout MEFs, lentivirus-mediated transduction with RECK-targeted shRNAs resulted in marked downregulaton of cell proliferation (Figure 1d). Furthermore, RECK depletion in such an acute manner upregulated $p19^{Arf}$, Trp53, $p21^{Cdkn1a}$ and $p16^{Ink4a}$ expression with reciprocal downregulation of Mdm2 within 48 h after shRNA transduction (Figure 1e). In the same experiment, we observed slight increase in Bax expression; however, we did not detect significant level of apoptosis in RECK-depleted MEFs by terminal deoxynucleotidyl transferase-mediated dUTP nick end labeling (TUNEL) (data not shown). These findings suggest that RECK controls cell proliferation by influencing on the ARF/Tp53/$p21^{Cdkn1a}$ pathway.

We eliminated the possibility of off-target effects by employing multiple sets of shRNA and appropriate controls. Moreover, whole cell lysates from live E9.5 *Reck*$^{-/-}$ embryos revealed marked induction of $p21^{Cdkn1a}$ (Figure 1f) and reciprocal downregulation of bromodeoxyuridine (BrdU) uptake (Figure 1g), both of which account for the smaller body size of *Reck*-nullizygous embryos (Oh *et al.*, 2001), indicating the genetic interaction between RECK and the ARF/Trp53/$p21^{Cdkn1a}$ pathway *in vivo*. Thus far, however, we have not found any evidence of either rescued or enhanced lethality in *Reck*$^{-/-}$ embryos at E10.5 by simultaneous *Cdkn1a* deletion (data not shown). In addition, *Reck*$^{-/-}$;*Cdkn1a*$^{-/-}$ MEFs exhibited accelerated proliferation rates, similar to *Reck*$^{+/+}$;*Cdkn1a*$^{-/-}$ MEFs on the 3T3 protocol assay (Figure S2). These findings suggest that *Cdkn1a* does not mediate the lethality caused by *Reck*-deficiency and that the effect of deletion of these two genes is not synthetic, i.e., their genetic relationship is linear.

Furthermore, 10 days after RECK depletion, we observed the evidence of cellular senescence in MEFs as assessed by increased senescence-associated β-galactosidase (SA-β-gal) activity, decreased BrdU uptake, increased $p16^{Ink4a}$ expression and nuclear accumulation of tri-methylated histone H3K9 (H3K9me3) (Figure 1h). We eliminated the possibility that RECK depletion induced apoptosis in MEFs even at 10 days after shRNA transduction by performing TUNEL staining (data not shown). In addition, we observed neither induction nor accumulation of γH2AX in these senesced cells (Figure 1i), eliminating the possibility that DNA damage response underlies the mechanism of

RECK depletion-induced cellular senescence. Additionally, we observed that RECK depletion in an adipogenic fibroblast cell line, PA6, caused an arrest of cell growth without promoting adipogenic differentiation, as assessed by Oil Red O staining, and the induction of PPARγ and C/EBPα (Figure S3a-b), eliminating the possibility that RECK depletion may cause premature differentiation in cultured fibroblast cells. In addition, we noticed that in contrast to MEFs under serum restriction, RECK is downregulated in PA6 cells under differentiation-inducing condition (Figure S3b).

RECK depletion-induced cellular senescence depends on Arf, Trp53 and Cdkn1a but not Ink4a

To study the mechanism by which RECK depletion induces growth suppression and cellular senescence, we infected MEFs on various genetic backgrounds with lentivirus expressing RECK shRNAs. *Arf*$^{-/-}$, *Trp53*$^{-/-}$ and *Cdkn1a*$^{-/-}$ but not *Ink4a*$^{-/-}$ MEFs were insensitive to RECK shRNA-induced growth suppression (Figure 2a) and cellular senescence (Figure 2b). In *Cdkn1a*$^{-/-}$ MEFs, we observed that RECK depletion did not induce p16^{Ink4a} (Figure 2c), suggesting that p16^{Ink4a} induction by RECK depletion depends on *Cdkn1a* loci. These findings suggest that RECK depletion-induced cellular senescence depends on *Arf*, *Trp53* and *Cdkn1a*.

RECK depletion induces transient upregulation of AKT and ERK activities through the elevation of EGFR activity

To further clarify the mechanism by which RECK depletion induces growth suppression and cellular senescence, we studied the activity of various intra-cellular signaling molecules. Since we discovered RECK originally as a gene that antagonized Ras-transformation in a cell phenotype-based cDNA screening (Takahashi et al., 1998), we particularly focused on Ras signaling. We identified increased phosphorylation of AKT and ERK, and upregulated expression of cyclin D1; all these were induced within 48 h after shRNA-mediated RECK depletion in MEFs (Figure 3a). To investigate the mechanism by which RECK functionally interacts with AKT and ERK, we tested numbers of inhibitors to various cellular signaling. We first conceived that RECK may modulate activity of receptors as we observed in our previous studies (Muraguchi et al., 2007; Miki et al., 2010). The increased phosphorylation of AKT and ERK induced by RECK depletion was sensitive to the receptor tyrosine kinase inhibitor genistein

(4',5,7-trihydroxyisoflavone) (Figure S4a). Since genistein inhibits broad range of receptor tyrosine kinases and others, we then examined more specific inhibitors. We found that gefitinib (N-(3-chloro-4-fluoro-phenyl)-7-methoxy-6-(3-morpholin-4-ylpropoxy)quinazolin-4-amine), a specific EGFR inhibitor, almost completely recapitulated the results obtained by genistein (Figure 3a). Consistent with these results, we observed increased EGFR phosphorylation within 2 days of RECK depletion with insignificant change in its protein amount (Figure 3b). The increased EGFR activity induced by RECK depletion was suppressed by both genistein (Figure S4b) and gefitinib (Figure 3b). These findings suggest that RECK depletion in an acute manner induces upregulation of AKT and ERK activities through the elevation of EGFR activity.

Mechanism of cellular senescence induced by shRNA-mediated RECK depletion

The induction of $p19^{Arf}$, Trp53 and $p21^{Cdkn1a}$ by RECK depletion was sensitive to both genistein (Figure S5a) and gefitinib (Figure 4a), indicating that RECK depletion upregulated these molecules through EGFR signaling modulation. Moreover, we observed that Sprouty 2 upregulation was associated with EGFR activation and attenuated by treatment with genistein (Figue S5b) or gefitinib (Figue 4b). Sprouty 2 is upregulated by Ras signaling and thereafter antagonizes Ras activation via negative feedback mechanism (Courtois-Cox *et al.*, 2006) at multiple points along the Ras regulatory pathway (Gross *et al.*, 2001; reviewed in Kim and Bar-Sagi, 2004). We monitored AKT and ERK activities in MEFs 10 days after shRNA transduction; as expected, these activities were strongly downregulated (Figure 4c). We further observed downregulated Ras activity in RECK-depleted cells (Figure 4d), confirming suppression of RAS signaling. We examined whether simultaneous depletion of Sprouty 2 is sufficient to block the effects of RECK depletion on RAS signaling; however, the result was negative (data not shown). We speculated that since the negative feedback mechanism to RAS signaling involves more than ten modulators of RAS signaling, i.e., several Ras-GAPs, Ras-GEFs, Sprouty and Spred family members, and dual specificity phosphatases (DUSPs), simultaneous depletion of solely Sprouty 2 was insufficient to antagonize RECK depletion in suppressing RAS signaling.

Furthermore, both genistein (Figue S5c) and gefitinib (Figure 4e) treatment partially but

significantly abrogated the negative impact of shRNA-mediated RECK depletion on cell growth. Altogether, these findings suggest that shRNA-mediated RECK depletion induces transient activation of AKT and ERK by enhancing EGFR activation; however, the stimuli to promote cell growth are antagonized by the induction of $p19^{Arf}$, Trp53 and $p21^{Cdkn1a}$, and the negative feedbacks to the Ras pathway including Sprouty 2 induction, subsequently leading to cellular senescence.

Overexpression of RECK attenuates Ras signaling in colon cancer cells

The abovementioned studies assessed the effects of loss of RECK function. We then assessed the effect of gain of RECK function on EGFR signaling. We first attempted to reconstitute RECK in *Reck*$^{-/-}$ MEFs and measure Ras signaling. We infected *Reck*$^{-/-}$ MEFs cultivated for approximately 10 passages with retrovirus vector carrying RECK cDNA (Miki et al., 2007), selected with blasticidin, and confirmed physiological level expression of RECK. However, we could not detect downregulation of Ras signaling in RECK-reconstituted *Reck*$^{-/-}$ MEFs (data not shown). We speculated that, in contrast to RECK depletion which induces irreversible withdrawal from cell cycle, the effect of gain of RECK function on Ras signaling in MEFs is reversible and adjustable. We also thought that the downregulation of Ras signaling may generate disadvantage in clonal expansion during drug selection thus it is difficult to demonstrate.

Nonetheless, we thought that the transient overexpression of RECK may enable us to observe its negative impact on RAS signaling. We screened number of non-transformaed and cancer-derived cell lines with relatively high transfection-competency to find out one that is sensitive to RECK. We finally found that transient overexpression of human RECK in SW480 colon cancer cells was sufficient to downregulate AKT and ERK activities and cyclinD1 expression, and upregulate $p21^{Cdkn1a}$ expression (Figure 5a). In addition, RECK overexpression significantly suppressed EGFR activity (Figure 5b). Altogether, the data obtained in this study indicate that RECK antagonizes Ras signaling through modulation of EGFR activation.

Treatment of MEFs by EGF and fibroblast growth factor (FGF) strongly attenuated RECK expression (Figure S6a), consistent with our previous finding that oncogenic Ras attenuates *Reck* transcription (Takahashi *et al.*, 1998) since both factors are well known

to stimulate Ras signaling. Taken together with other results, we propose that the RECK and Ras signals are mutually suppressing (Figure S6b).

Mechanism of the RECK-EGFR genetic interaction

Finally, we addressed the mechanistic aspects of the RECK-EGFR genetic interaction. The exogenous introduction of wild type RECK-expression vector that is insensitive to our RECK shRNAs antagonized the effect of endogenous RECK depletion on cell growth (Figure 6a-b). This again eliminated the possibility that the effects of RECK shRNAs on cell proliferation were the product of off-target effects. Interestingly, in the same setting, secreted form of RECK (RECKΔC: one mutant lacking the membrane anchor) was unable to antagonize RECK shRNAs, indicating that membrane-anchoring is required for RECK modulation of cell growth mediated by Ras signaling (Figure 6a-b). We have thus far been unable to detect a direct interaction between RECK and EGFR (data not shown).

Next, we hypothesized that increased metallo-endopeptidase activities induced by RECK loss may affect cell growth and Ras signaling in MEFs. However, a broad spectrum (non-specific) metallo-endopeptidase inhibitor, GM6001, did not show antagonism to Ras signaling activation and growth arrest induced by RECK depletion (Figure 7a-b). Then, we assessed specifically the MMP-2 and MT1-MMP-dependency of RECK function in Ras signaling modulation, as it had been previously addressed in the context of embryonic development (Oh *et al.*, 2001), endocytosis (Miki et al., 2007) and vascular development (Miki et al., 2010). We first examined whether germ-line loss of MMP-2 or MT1-MMP antagonizes RECK depletion-induced growth suppression. Both *MMP-2*$^{-/-}$ MEFs and *MT1-MMP*$^{-/-}$ MEFs exhibited partial but significant resistance to RECK depletion-induced growth suppression (Figure 7c). More importantly, suppression of RAS signaling by RECK depletion was significantly lesser in those MEFs than in wild type (Figure 7d). These findings suggest that MT1-MMP/MMP-2 system may mediate RECK to modulate EGFR signaling.

We finally addressed whether in other lineage of cells, RECK depletion-induced cellular senescence associates with Ras signaling downregulation in an MMP-2-dependent manner. Human umbilical endothelial cells (HUVECs) express MMP-2 (Jodele *et al.*,

2006). Our recent study has demonstrated that siRNA-mediated RECK depletion in HUVECs induced proliferation defects and abnormal vascular development in part in an MMP-2-dependent manner (Miki *et al.,* 2010). In consistent with our current study using MEFs, siRNAs targeting RECK induced upregulation of Sprouty 2, and reciprocal downregulation of ERK activity in HUVECs at 3 days after transduction; these were significantly antagonized by simultaneous introduction of MMP-2 siRNAs (Figure S7a). In consonance, the growth suppression in HUVECs induced by RECK depletion was partially antagonized by simultaneous MMP-2 depletion (Figure S7b). These findings suggest a specific role of MMP-2 in the RECK-EGFR genetic interaction in multiple lineages of cells.

Discussion

In this study, the functions of RECK in cultured cells (MEFs, colon cancer cells and vascular endothelial cells) and embryos were assessed by a variety of 'loss of function' and 'gain of function' investigations. We concluded that RECK antagonizes Ras signaling via attenuating EGFR activation in multiple cell lineages. The precise mechanism of the RECK-EGFR genetic interaction and its dependency on MMP-2 and MT1-MMP is currently under intensive investigation. MMP-2 or MT1-MMP may indirectly influence on the ectodomain shedding of membrane-tethered growth factors binding to EGFR family members that is thought to be mediated by a disintegrin and metalloprotease (ADAM) members. However, so far, we did not observe change in the degree of ectodomain shedding of EGFR family ligands (TGFα, EGF, HB-EGF, Betacellulin, Amphiregulin and Epiregulin) by modulating RECK expression (data not shown), and we so far did not detect direct binding of RECK and EGFR.

Despite the marked induction of $p21^{Cdkn1a}$ observed in whole embryos, MEFs separated from E10.0 *Reck*$^{-/-}$ embryos expressed $p21^{Cdkn1a}$ at a level comparable to wild type cells, suggesting that *Reck*-deficiency causes a certain stress to the whole body, leading to $p21^{Cdkn1a}$ induction, or that $p21^{Cdkn1a}$ level had been quickly adjusted to normal level under *in vitro* culture conditions during 3 passages. Acquirement of accelerated and immortal cell proliferation by *Reck*$^{-/-}$ MEFs during successive cell cultivation was closely correlated with attenuated $p19^{Arf}$, Trp53 and $p21^{Cdkn1a}$ expression. In contrast,

RECK depletion-induced cellular senescence required the presence of these loci. These seemingly self-contradicting findings helped us to conceive that the cellular signaling modulated by RECK could be bivalent in the control of cell proliferation. We then noticed that the notion of 'oncogene-induced senescence' (Collado and Serrano, 2010) and its revised version notion 'negative feedback to Ras signaling' (Courtois-Cox *et al.*, 2008) may explain our findings.

Cellular senescence induced by oncogenic Ras has been proposed to be mediated by DNA hyper-replication and following DNA damage response (Bartkova *et al.*, 2006; Di Micco *et al*., 2006); this may explain RECK depletion-induced cellular senescence. However, we eliminated this possibility by investigating several markers of DNA damage response including γH2AX (Figure 1i) and phosphorylated $Trp53^{S15}$ (data not shown) in RECK-depleted MEFs. Also, the positive sensitivity of *Ink4a*$^{-/-}$ MEFs to RECK depletion-induced cellular senescence may imply that the nature of Ras activation induced by RECK depletion differs from that of oncogenically mutated Ras. We further speculate that DNA damage may be prerequisite for $p16^{Ink4a}$-dependent but not for ARF/p53/$p21^{Cdkn1a}$ -dependent cellular senescence induced by oncogenic stimuli.

The relationship between *RECK* and *Sprouty 2* is highly similar to that initially noted between the *Neurofibromatosis type 1* (*NF1*) tumor suppressor gene and *Sprouty 2* (Courtois-Cox *et al.*, 2006). NF1 is a member of the Ras GTPase activating proteins (RasGAPs) that suppresses Ras activation by promoting hydrolysis of GTP (reviewed in Cichowski and Jacks, 2001). Activation of Ras signaling induced by NF1 inactivation provokes a series of negative feedback loops to Ras pathways by inducing the transactivation of many of antagonists to Ras signaling pathway including the Sprouty (suppressor of Ras) and SPRED (Sprouty-related protein) family members, and many of RasGAPs and dual specificity phosphatases (DUSPs), in an AKT/FOXO- and Rb/Trp53-dependent manner (Courtois-Cox *et al.*, 2006). Cichowski's research group thereby revised the "oncogene-induced cellular senescence model" (Serrano *et al.*, 1997) by proposing this negative feedback mechanism (Bardeesy and Sharpless, 2006). We observed this mechanism in cells that acutely lost RECK function, highlighting the tumor suppressor trait of *RECK* gene more clearly than ever. We also speculate that in contrast to the shRNA-mediated RECK depletion, the germ-line *RECK* knockout

allowed cells to take enough time to override growth-suppressing signals involving negative feedback pathway before cellular senescence program was engaged. We are currently examining whether early escape from cellular senescence by *Reck*$^{-/-}$ MEFs depends on EGFR function.

The strong clinical relevance of the tumor suppressor trait of *RECK* gene had been previously provided by a couple of studies that reported strong correlations between RECK expression and favorable prognosis for patients with non-small-cell lung cancer (NSCLC) (Takenaka *et al.*, 2004; Takenaka *et al.*, 2005) whose malignant behaviors critically depend on EGFR signaling (reviewed in Andratschke *et al.*, 2004; Jänne *et al.*, 2005). In addition to NSCLC, RECK significantly predicts favorable prognosis in many types of cancer including colorectal cancer (Rahmah *et al.*, 2009; Long *et al.*, 2008; Takemoto *et al.*, 2007; Rabien *et al.*, 2007; refs in Clark, 2007; refs in Noda and Takahashi, 2007). Our current study demonstrated that RECK attenuates AKT and ERK in the SW480 colon cancer cell line overriding the activating mutation in K-*ras* harbored by this cell line (Anker *et al.*, 1994). We originally identified RECK as a gene product whose overexpression dominantly antagonizes oncogenic K-*ras*-induced transformation (Takahashi *et al.*, 1998). Altogether, our current study suggests that RECK antagonizes both physiological and oncogenic Ras signaling.

RECK transcription is suppressed by oncogenic Ras (Takahashi *et al.*, 1998). As expected, the treatment of cells with EGF and FGF strongly suppressed RECK expression in cell culture (Figure S6a). In this study, mutual suppression between RECK and Ras signaling was demonstrated (Figure S6b). In addition, many of retroviral oncogenes (Takahashi *et al.*, 1998), oncogenic DNA virus products (Liu *et al.*, 2003) and the so-called ‘oncomir’ (oncogenic microRNA) miR-21 (Hu *et al.*, 2008; Gabriely *et al.*, 2008; Zhang *et al.*, 2008; Loayza-Puch *et al*., 2010; reviewed in Nicoloso *et al*, 2009) were demonstrated to negatively regulate RECK transcription. These findings indicate that these oncogenic signals may commonly impact on Ras signaling from the extracellular space via transcriptional regulation of RECK.

It was demonstrated that MMP-9 is transcriptionally regulated by RECK via transcription factors Fra-1 and c-Jun through 12-*O*-tetradecanoylphorbol-13-acetate

(TPA)-responsive (TRE)-1 site in the MMP-9 promoter (Takagi *et al.*, 2009). Fra-1 and c-Jun are highly established downstream targets of EGFR signaling, and MMP-9 is indeed upregulated by EGF (Lyons *et al.*, 1993). There is a possibility that RECK directs MMP-9 transcription by modulating EGFR signaling. In addition, we recently determined that RECK is a direct substrate of several MMP activities (Takegami *et al.*, in preparation for publication). It is possible that MMP activities enhance Ras signaling even by impairing RECK functions. We further speculate that RECK may function as a converter of extracellular protease activities to Ras signaling.

Finally, this study demonstrated that like loss of *Phosphatase and Tensin Homolog Deleted from Chromosome 10* (*PTEN), NF1* or *Von Hippel-Lindau disease* (*VHL*) tumor suppressor genes (Chen *et al.*, 2005; Courtois-Cox *et al.*, 2006; Young *et al.*, 2008), or activating mutation in several *Ras* isoforms or B-*Raf* (Braig *et al.*, 2005; Michaloglou *et al.*, 2005), the effect of loss of RECK function on cell proliferation is counteracted by the cellular senescence program. Furthermore, we have recently reported that carcinogenesis induced by loss of the *Retinoblastoma* (*Rb*) tumor suppressor gene is antagonized by DNA damage response and cellular senescence induced by E2F-depednent activation of N-Ras (Shamma *et al.*, 2009). Therefore, we speculate that signals antagonistic to loss of many tumor suppressors may commonly converge on Ras signaling.

Materials and Methods

Mice

Reck$^{+/-}$ mice (Oh *et al*., 2001) were backcrossed to C57BL/6 mice for 6 generations, and intercrossed for timed pregnancy. *Arf* knockout mice were gifted from T. Kamijo (Kamijo *et al.*, 1997). *Trp53* knockout mice (Tsukada *et al*., 1993) were obtained from RIKEN BRC (Acc. No. CDB0001K). *Cdkn1a* knockout mice were gifted from P. Leder (Deng *et al.*, 1995). *Ink4a* knockout mice were from N. Sharpless (Sharpless *et al.*, 2001). *MMP2* knockout mice were from S. Itohara (Itoh *et al*., 1997) and *MT1-MMP* knockout mice were from Y. Okada and M. Seiki (Oh *et al.*, 2004). Animals were handled in accordance with the guidelines of Kyoto University and Kanazawa University.

Generation of MEFs

Primary MEFs were prepared as described previously (Shamma *et al.*, 2009) from individual embryos of various genotypes, and maintained in α-Modified Eagle's Medium (α-MEM) supplemented with 10% fetal bovine serum (FBS). Primary MEFs were used for each experiment before 10 passages.

3T3 protocol

2 x 10^5 cells were plated in 60 mm diameter dishes. After 3 days, the total number of cells in each dish was counted using a particle counter (Coulter Counter Z1, Beckman Coulter), and 2 x 10^5 cells were re-plated into the 60 mm diameter dishes. This procedure was repeated every 3 days for 20~30 passages.

Retrovirus and plasmids

Retroviruses were recovered from Ecopack293-2 (Clontech) transfected with pLXSB, pLXSB-human RECK (hRECK) (Miki *et al.*, 2007), pLXSB-hRECKΔC (Takahashi *et al*., 1998), pBabe-puro, and pBabe-puro-p21. MEFs were plated 20 h before infection, and infected with virus in the presence of 8 μg/ml polybrene. The estimated multiplicity of infection (MOI) was 2 to 3. Twenty-four hours after infection, infected cells were selected in the presence of 8 μg/ml blasticidin or 2 μg/ml puromycin.

RNA interference

MISSION TRC shRNA target sets for mouse RECK (*sh*-RECK #1: TRCN80129 and *sh*-RECK #2: TRCN80131), those targeting Luciferase (*sh*-Luciferase: SHC007) and negative control (*sh*-Negative control: SHC002) were purchased from Sigma-Aldrich. Generation and infection of lentivirus were performed according to the manufacturer's instruction.

Proliferation assay

Cells were plated on 96 well-type plates (1 x 10^3 cells/well). After shRNA-lentivirus infection, the cell numbers were quantified by colorimetric assay using Cell count reagent SF (07553-15, Nacalai tesque, Japan) according to the manufacturer's instructions.

Immunoblotting and Immunofluorescence

Immunoblotting and immunofluorescence were performed in buffer (Miki et al., 2007) or in acid-extraction buffer (Shamma et al., 2009) as described previously using the following antibodies: $p19^{Arf}$ (#07-543, Upstate), Trp53 (1C12, Cell Signaling Technology), $p21^{CDKN1A}$ (#556430, BD bioscience), α-Tubulin (Ab-1, Calbiochem), RECK (Miki et al., 2007), Mdm2 (4B11, Calbiochem), Bax (sc-493, Santa Cruz Biotechnology), $p16^{INK4a}$ (sc-1207, Santa Cruz Biotechnology), H3K9me3 (#07-442, Upstate), γH2AX (#05-636, Upstate), Phosphorylated AKT (#9271, Cell Signaling Technology), Total-AKT (#9272, Cell Signaling Technology), Phosphorylated ERK1/2 (#9101, Cell Signaling Technology), Total-ERK1/2 (#9102, Cell Signaling Technology), cyclinD1 (DCS6, Cell Signaling Technology), EGFR (#06-847, Upstate), Sprouty 2 (sc-30049, Santa Cruz Biotechnology), and Ras (#610002, BD bioscience).

BrdU incorporation

Cultured cells were incubated with 10 μM BrdU for 60 min. The *in utero* BrdU labeling of E10.0 embryos was performed as described previously (Muraguchi *et al.*, 2007). For embryo labeling, the tissue was dispersed by 0.25 % Trypsin/EDTA for 5 min at room temperature. Samples were stained using the BrdU Labeling and Detection Kit l (Cat.No.1 296 736, Roche Diagnostics) according to the manufacture's instructions. Data were collected using FACS Aria (BD Biosciences).

SA-β-gal staining

Cells were fixed with 0.2 % glutaraldehyde and 0.2 % formaldehyde in phosphate-buffered saline (PBS) (pH7.5), and stained in SA-β-gal solution (1 mg/ml X-gal, 5 mM $K_3Fe(CN)_6$, 5 mM $K_4Fe(CN)_6$, and 2 mM $MgCl_2$ in PBS (pH6.0)) for 12 h at 37 ^{O}C.

Immunoprecipitation

Cell lysates were prepared as described previously (Miki *et al.*, 2007). Proteins with phosphorylated tyrosine were immunoprecipitated using anti-phosphorylated Tyrosine (pTyr) antibody (PY99, Santa Cruz Biotechnology). The immunoprecipitates were collected on protein A-agarose beads (20334, Pierce), washed 5 times with lysis buffer,

eluted, and analyzed by immunoblotting.

Ras activation assay

Cell lysates were prepared as described previously (Shamma *et al.*, 2009). 500 μg of the lysates were incubated with the Ras binding domain (RBD) of cRaf-1 fused to glutathione S-transferase (GST) to precipitate GTP-loaded Ras. Glutathione-Sepharose 4B (17-0756-01, GE healthcare) beads were preloaded with GST-RBD. After incubation at 4°C for 1 h, beads were washed 5 times with lysis buffer, eluted, and analyzed by immunoblotting.

Transient trasfection

Cells were transfected with pCXN2, or pCXN2-hRECK (Takahashi et al., 1998) using CalPhos™ Mammalian Transfection Kit (631312, Clontech) according to the manufacturer's instructions.

Acknowledgments

We thank H. Sato and T. Muraguchi for critical reading of the manuscript; T. Kamijo, P. Leder, N. Sharpless, S. Itohara, Y. Okada and M. Seiki for providing mice; M. Seiki, T. Sakamoto and T. Nakano for providing cells; S. Yano and K. Matsumoto and S. Higashiyama for providing reagent, C. Sugita for supporting mouse transfer; W. Hung, K. Lee and J. Oh for encouragement; H. Gu and A. Nishimoto for technical assistance; and A. Miyazaki and M. Suzuki for secretarial assistance. SK thanks the JASSO scholarship for support. This work was supported by a Research Grant of the Princess Takamatsu Cancer Research Fund, Astellas Foundation for Research on Metabolic Disorders, the Takeda Science Foundation, and the Japanese Ministry of Education, Culture, Sports, Science and Technology.

References

Anker P, Lyautey J, Lefort F, Lederrey C and Stroun M. (1994). C R Acad Sci III, 317, 869-74.

Bardeesy N and Sharpless NE. (2006). Cancer Cell, 10, 451-3.

Bartkova J, Rezaei N, Liontos M, Karakaidos P, Kletsas D, Issaeva N, Vassiliou LV, Kolettas E, Niforou K, Zoumpourlis VC, Takaoka M, Nakagawa H, Tort F, Fugger K, Johansson F, Sehested M, Andersen CL, Dyrskjot L, Orntoft T, Lukas J, Kittas C, Helleday T, Halazonetis TD, Bartek J and Gorgoulis VG. (2006). Nature, 444, 633-7.

Braig M, Lee S, Loddenkemper C, Rudolph C, Peters AH, Schlegelberger B, Stein H, Dorken B, Jenuwein T and Schmitt CA. (2005). Nature, 436, 660-5.

Chang HC, Cho CY and Hung WC. (2006). Cancer Res, 66, 8413-20.

Chang HC, Cho CY and Hung WC. (2007). Cancer Sci, 98, 169-73.

Chang HC, Liu LT and Hung WC. (2004). Cell Signal, 16, 675-9.

Chen Z, Trotman LC, Shaffer D, Lin HK, Dotan ZA, Niki M, Koutcher JA, Scher HI, Ludwig T, Gerald W, Cordon-Cardo C and Pandolfi PP. (2005). Nature, 436, 725-30.

Cichowski K and Jacks T. (2001). Cell, 104, 593-604.

Clark JC, Thomas DM, Choong PF and Dass CR. (2007). Cancer Metastasis Rev, 26, 675-83.

Collado M and Serrano M. (2010). Nat Rev Cancer, 10, 51-7.

Courtois-Cox S, Genther Williams SM, Reczek EE, Johnson BW, McGillicuddy LT, Johannessen CM, Hollstein PE, MacCollin M and Cichowski K. (2006). Cancer Cell, 10, 459-72.

Courtois-Cox S, Jones SL and Cichowski K. (2008). Oncogene, 27, 2801-9.

D'Souza B, Miyamoto A and Weinmaster G. (2008). Oncogene, 27, 5148-67.

Deng C, Zhang P, Harper JW, Elledge SJ and Leder P. (1995). Cell, 82, 675-84.

Di Micco R, Fumagalli M, Cicalese A, Piccinin S, Gasparini P, Luise C, Schurra C, Garre M, Nuciforo PG, Bensimon A, Maestro R, Pelicci PG and d'Adda di Fagagna F. (2006). Nature, 444, 638-42.

Gabriely G, Wurdinger T, Kesari S, Esau CC, Burchard J, Linsley PS and Krichevsky AM. (2008). Mol Cell Biol, 28, 5369-80.

Gross I, Bassit B, Benezra M and Licht JD. (2001). J Biol Chem, 276, 46460-8.

Hatta M, Matsuzaki T, Morioka Y, Yoshida Y and Noda M. (2009). Cell Signal, 21, 1885-93.

Hu SJ, Ren G, Liu JL, Zhao ZA, Yu YS, Su RW, Ma XH, Ni H, Lei W and Yang ZM. (2008). J Biol Chem, 283, 23473-84.

Itoh T, Ikeda T, Gomi H, Nakao S, Suzuki T and Itohara S. (1997). J Biol Chem, 272, 22389-92.

Jodele S, Blavier L, Yoon JM and DeClerck YA. (2006). Cancer Metastasis Rev, 25, 35-43.

Kamijo T, Zindy F, Roussel MF, Quelle DE, Downing JR, Ashmun RA, Grosveld G and Sherr CJ. (1997). Cell, 91, 649-59.

Kim HJ and Bar-Sagi D. (2004). Nat Rev Mol Cell Biol, 5, 441-50.

Liu LT, Peng JP, Chang HC and Hung WC. (2003). Oncogene, 22, 8263-70.

Loayza-Puch F, Yoshida Y, Matsuzaki T, Takahashi C, Kitayama H and Noda M. (2010). Oncogene, 29, 2638-48.

Long NK, Kato K, Yamashita T, Makita H, Toida M, Hatakeyama D, Hara A, Mori H and Shibata T. (2008). Oral Oncol, 44, 1052-8.

Lyons JG, Birkedal-Hansen B, Pierson MC, Whitelock JM and Birkedal-Hansen H. (1993). J Biol Chem, 268, 19143-51.

Michaloglou C, Vredeveld LC, Soengas MS, Denoyelle C, Kuilman T, van der Horst CM, Majoor DM, Shay JW, Mooi WJ and Peeper DS. (2005). Nature, 436, 720-4.

Miki T, Takegami Y, Okawa K, Muraguchi T, Noda M and Takahashi C. (2007). J Biol Chem, 282, 12341-52.

Miki T, Shamma A, Kitajima S, Takegami Y, Noda M, Nakashima Y, Watanabe K and Takahashi C. (2010). Mol. Cancer Res, 8, 665-76.

Morioka Y, Monypenny J, Matsuzaki T, Shi S, Alexander DB, Kitayama H and Noda M. (2009). Oncogene, 28, 1454-64.

Muraguchi T, Takegami Y, Ohtsuka T, Kitajima S, Chandana EP, Omura A, Miki T, Takahashi R, Matsumoto N, Ludwig A, Noda M and Takahashi C. (2007). Nat Neurosci, 10, 838-45.

Nicoloso MS, Spizzo R, Shimizu M, Rossi S and Calin GA. (2009). Nat Rev Cancer, 9, 293-302.

Noda M and Takahashi C. (2007). Cancer Sci, 98, 1659-65.

Oh J, Takahashi R, Kondo S, Mizoguchi A, Adachi E, Sasahara RM, Nishimura S, Imamura Y, Kitayama H, Alexander DB, Ide C, Horan TP, Arakawa T, Yoshida H, Nishikawa S, Itoh Y, Seiki M, Itohara S, Takahashi C and Noda M. (2001). Cell, 107, 789-800.

Oh J, Takahashi R, Adachi E, Kondo S, Kuratomi S, Noma A, Alexander DB, Motoda H,

Okada A, Seiki M, Itoh T, Itohara S, Takahashi C and Noda M. (2004). Oncogene, 23, 5041-8.

Omura A, Matsuzaki T, Mio K, Ogura T, Yamamoto M, Fujita A, Okawa K, Kitayama H, Takahashi C, Sato C and Noda M. (2009). J Biol Chem, 284, 3461-9.

Rabien A, Burkhardt M, Jung M, Fritzsche F, Ringsdorf M, Schicktanz H, Loening SA, Kristiansen G and Jung K. (2007). Eur Urol, 51, 1259-66.

Rahmah NN, Sakai K, Nakayama J and Hongo K. (2009). Neurosurg Rev.

Sasahara RM, Takahashi C and Noda M. (1999). Biochem Biophys Res Commun, 264, 668-75.

Serrano M, Lin AW, McCurrach ME, Beach D and Lowe SW. (1997). Cell, 88, 593-602.

Shamma A, Takegami Y, Miki T, Kitajima S, Noda M, Obara T, Okamoto T and Takahashi C. (2009). Cancer Cell, 15, 255-69.

Sharpless NE, Bardeesy N, Lee KH, Carrasco D, Castrillon DH, Aguirre AJ, Wu EA, Horner JW and DePinho RA. (2001). Nature, 413, 86-91.

Takagi S, Simizu S and Osada H. (2009). Cancer Res, 69, 1502-8.

Takahashi C, Sheng Z, Horan TP, Kitayama H, Maki M, Hitomi K, Kitaura Y, Takai S, Sasahara RM, Horimoto A, Ikawa Y, Ratzkin BJ, Arakawa T and Noda M. (1998). Proc Natl Acad Sci U S A, 95, 13221-6.

Takenaka K, Ishikawa S, Kawano Y, Yanagihara K, Miyahara R, Otake Y, Morioka Y, Takahashi C, Noda M, Wada H and Tanaka F. (2004). Eur J Cancer, 40, 1617-23.

Takenaka K, Ishikawa S, Yanagihara K, Miyahara R, Hasegawa S, Otake Y, Morioka Y, Takahashi C, Noda M, Ito H, Wada H and Tanaka F. (2005). Ann Surg Oncol, 12,

817-24.

Todaro GJ and Green H. (1963). J Cell Biol, 17, 299-313.

Tsukada T, Tomooka Y, Takai S, Ueda Y, Nishikawa S, Yagi T, Tokunaga T, Takeda N, Suda Y, Abe S, Matuso I, Ikwa Y and Aizawa S. (1993). Oncogene, 8, 3313-22.

Young AP, Schlisio S, Minamishima YA, Zhang Q, Li L, Grisanzio C, Signoretti S and Kaelin WG, Jr. (2008). Nat Cell Biol, 10, 361-9.

Zhang Z, Li Z, Gao C, Chen P, Chen J, Liu W, Xiao S and Lu H. (2008). Lab Invest, 88, 1358-66.

Zolkiewska A. (2008). Cell Mol Life Sci, 65, 2056-68.

Figure legends

Figure 1 Effects of germ-line knockout and shRNA-mediated depletion of RECK in MEFs.

(a) 3T3 protocol assay of MEFs of the indicated genotypes. WT: wild type littermate. Cumulative multiplicity (log10) in the representative cultures at the indicated passage numbers is shown.

(b) Immunoblotting (IB) of the indicated proteins in MEFs of the indicated genotype at passage number 3 (upper) and 15 (lower).

(c) *Reck*$^{-/-}$ MEFs at passage number 22 were retrovirally transduced with pBabe-puro or pBabe-puro-p21^{CDKN1A} and selected. The 3T3 protocol assay of the resultant cells is shown (left). IB of the indicated proteins in the resultant cells (right).

(d) Relative number of MEFs lentivirally transduced with the indicated shRNAs and cultured for 5 days was quantified by colorimetric assay. Bars are means ± SEM (n = 3).

(e) IB of the indicated proteins in whole cell lysates from MEFs transduced with the indicated shRNAs and cultured for 48 h.

(f) IB of the indicated proteins in E9.5 mouse embryos of the indicated genotype. Three

pairs of littermate were analyzed.

(g) BrdU incorporation by E10.0 mouse embryos. Bars are means + SEM (n = 5 embryos of each genotype). *P < 0.01 by Student's *t*-test.

(h) Upper panels show SA-β-gal activity and BrdU incorporation in MEFs at 10 days after transduction with the indicated shRNAs (left). The frequency of cells with positive signal was quantified (right). Lower panels show immunofluorescence (IF) analysis of the indicated proteins in MEFs at 10 days after transduction with the indicated shRNAs. The frequency of cells with positive signal was quantified (right). Scale bar: 100 μm. Bars are means + SEM (n = at least 10 fields). The insets show high-power magnification pictures of signal-positive cells. Non: Non-Target.

(i) IF analysis of γH2AX in MEFs at 48 h after transduction with the indicated shRNAs. UV: Ultra Violet (germicidal lamp)-exposed for 30 min as positive control of DNA damage response. Scale bar: 100 μm. The insets show high-power magnification pictures of signal-positive cells.

Figure 2 Effects of shRNA-mediated RECK depletion on MEFs of different genetic backgrounds.

(a) Relative cell numbers of the indicated genotype of MEFs were quantified at 5 days after transduction with the indicated shRNAs. Bars are means + SEM (n = 3). *P < 0.01 by Student's *t*-test.

(b) SA-β-gal activity was detected (left) and quantified (right) in MEFs of the indicated genotype at 10 days after transduction with the indicated shRNAs. Scale bar: 200 μm. Bars are means + SEM (n = at least 10 fields).

(c) IB of the indicated proteins in whole cell lysates from the indicated genotype of MEFs transduced with the indicated shRNAs and cultured for 48 h.

Figure 3 Effects of shRNA-mediated RECK depletion on EGFR signaling in MEFs.

(a) IB of the indicated proteins in wild type MEFs transduced with the indicated shRNAs and cultured for 48 h in the presence of 0.1 % dimethyl sulfoxide (DMSO) (vehicle) or 1 μM gefitinib (S1025, Selleck Chemicals).

(b) Immunoprecipitation from whole lysates of cells from panel (a) with an anti-phosphorylated Tyrosine (pTry) antibody. Precipitates from 500 μg protein in

whole cell lysates (upper) or 20 μg protein in whole cell lysates (lower) were analyzed by IB with anti-EGFR antibody.

Figure 4 Negative feedback to RAS signaling induced by shRNA-mediated RECK depletion.

(a, b) IB of the indicated proteins in wild type MEFs transduced with the indicated shRNAs for and cultured for 48 h in the presence of 0.1 % DMSO (vehicle) or 1 μM gefitinib.

(c) IB of the indicated proteins in whole cell lysates from MEFs transduced with the indicated shRNAs and cultured for 10 days.

(d) Pull-down of GTP-loaded Ras from 500 μg protein in whole cell lysates (upper) or 20 μg protein in whole cell lysates (lower) were analyzed by IB with anti-Ras antibody. Whole cell lysates were prepared from MEFs transduced with the indicated shRNAs and cultured for 48 h.

(e) Relative numbers of MEFs at 5 days after transduction with the indicated shRNAs and treatment with 0.1 % DMSO (vehicle) or 1 μM gefitinib were quantified. Bars are means + SEM (n = 3). *P < 0.01 by Student's *t*-test.

Figure 5 Effects of RECK overexpression on EGFR signaling in colon cancer cells.

(a) SW480 cells were transiently transfected with pCXN2 (Vector) or pCXN2-human RECK cDNA (RECK) and cultured for 48 h. The expression of the indicated proteins in asynchronously growing transfectants was analyzed by IB.

(b) Immunoprecipitation from whole lysates of cells from panel (a) with an anti-pTyr antibody. Precipitates from 500 μg protein in whole cell lysates (upper) or 20 μg protein in whole cell lysates (lower) were analyzed by IB with anti-EGFR antibody. The relative activity of EGFR (phophorylated form per total) is quantified and indicated as control set to 1.0.

Figure 6 The membrane-anchoring-dependent function of RECK.

(a) RECK expression in MEFs retrovirally transduced with pLXSB, pLXSB-hRECK or pLXSB-RECKΔC and selected was analyzed by IB. WCL: whole cell lysates.

(b) Cells from panel (a) were then transduced with the indicated shRNAs. Relative cell

number was quantified at 5 days after transduction. Bars are means + SEM (n = 3). *P < 0.01 by Student's *t*-test.

Figure 7 The MMP-2 and MT1-MMP-dependent effect of RECK depletion on MEFs.

(a) IB of the indicated proteins in whole cell lysates from MEFs transduced with the indicated shRNAs and cultured for 48 h in the presence of 10μM GM6001 negative control (an ineffective analogue: #364210, Calbiochem) or 10 μM GM6001 (#364205, Calbiochem).

(b) MEFs transduced with the indicated shRNAs were incubated in growth medium containing either 10μM GM6001 negative control or 10μM GM6001. Relative cell number was counted at 5 days after transduction of the indicated shRNAs. Bars are means + SEM (n = 3).

(c) Cell proliferation of the indicated genotype of MEFs infected with lentivirus expressing the indicated shRNAs. Resultant cells were plated at 2 x 10^5 cells onto 60 mm dish, cultured for 4 days and photographed (left), and numbers of cells were quantified (right). Scale bar: 250 μm. Bars are means + SEM (n = 4 fields). *P < 0.01 by Student's *t*-test.

(d) IB of the indicated proteins in whole cell lysates from the indicated genotype of MEFs transduced with the indicated shRNA, selected and cultured for 4 days.

Kitajima et al., Figure 1 a-e

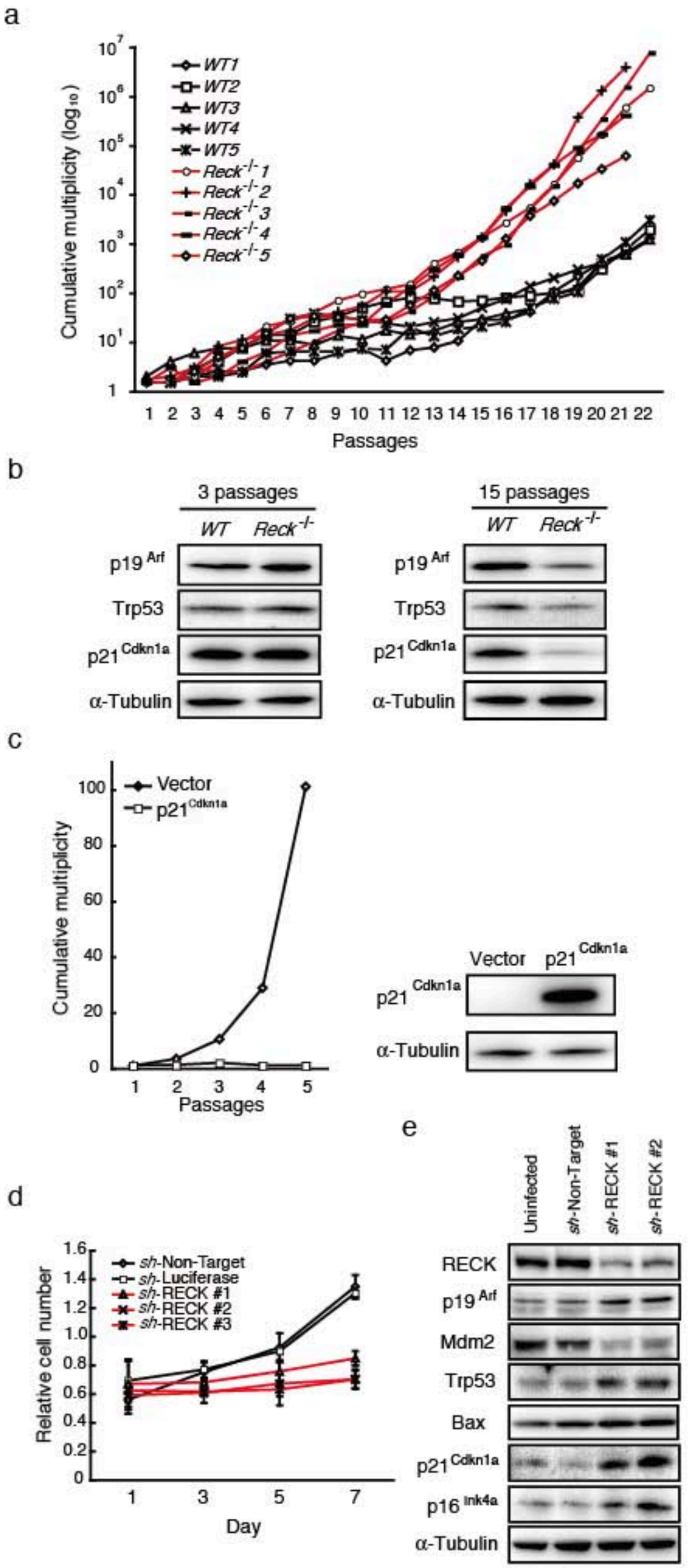

Kitajima et al., Figure 1 f-i

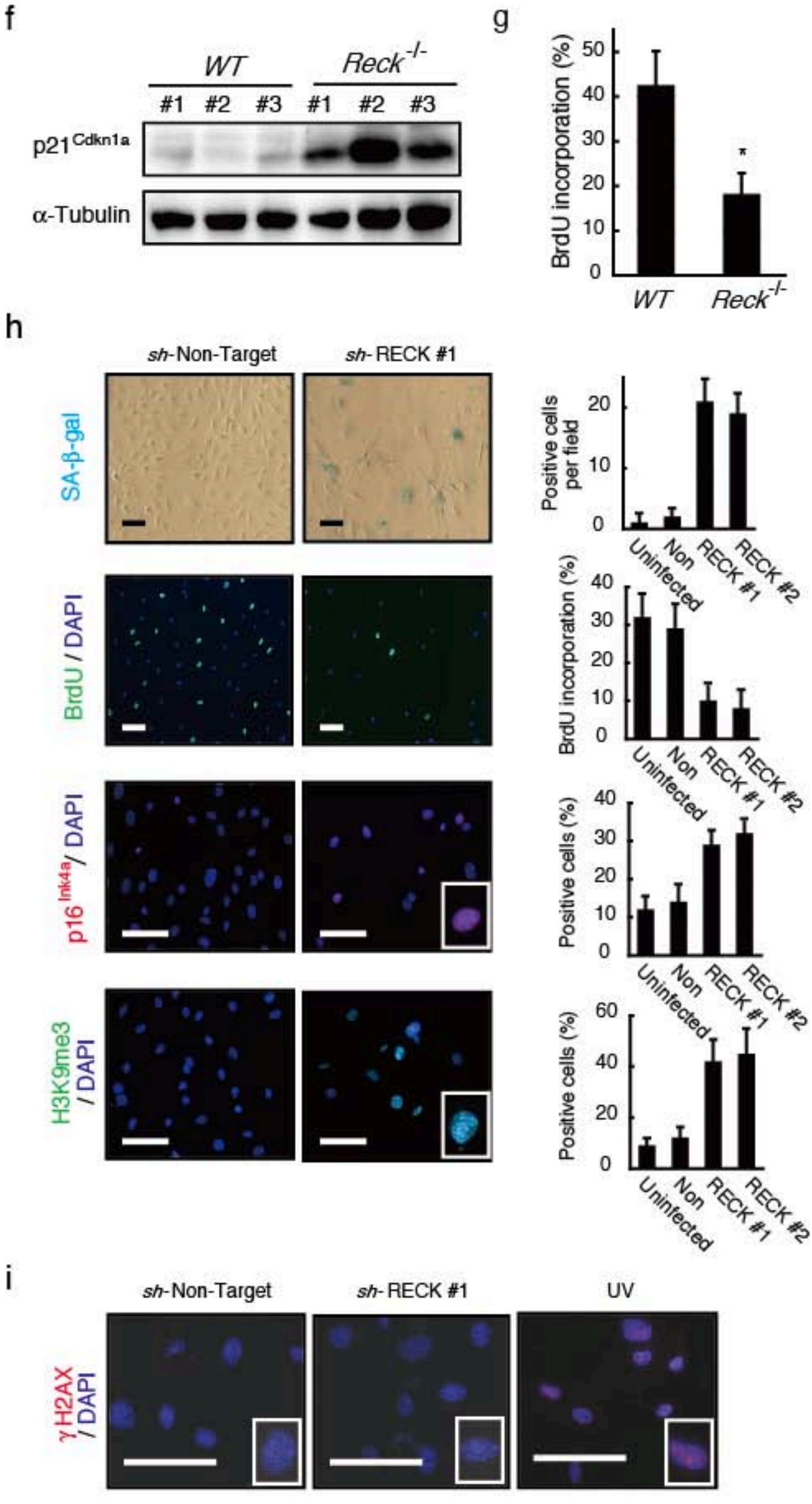

Kitajima et al., Figure 2

a

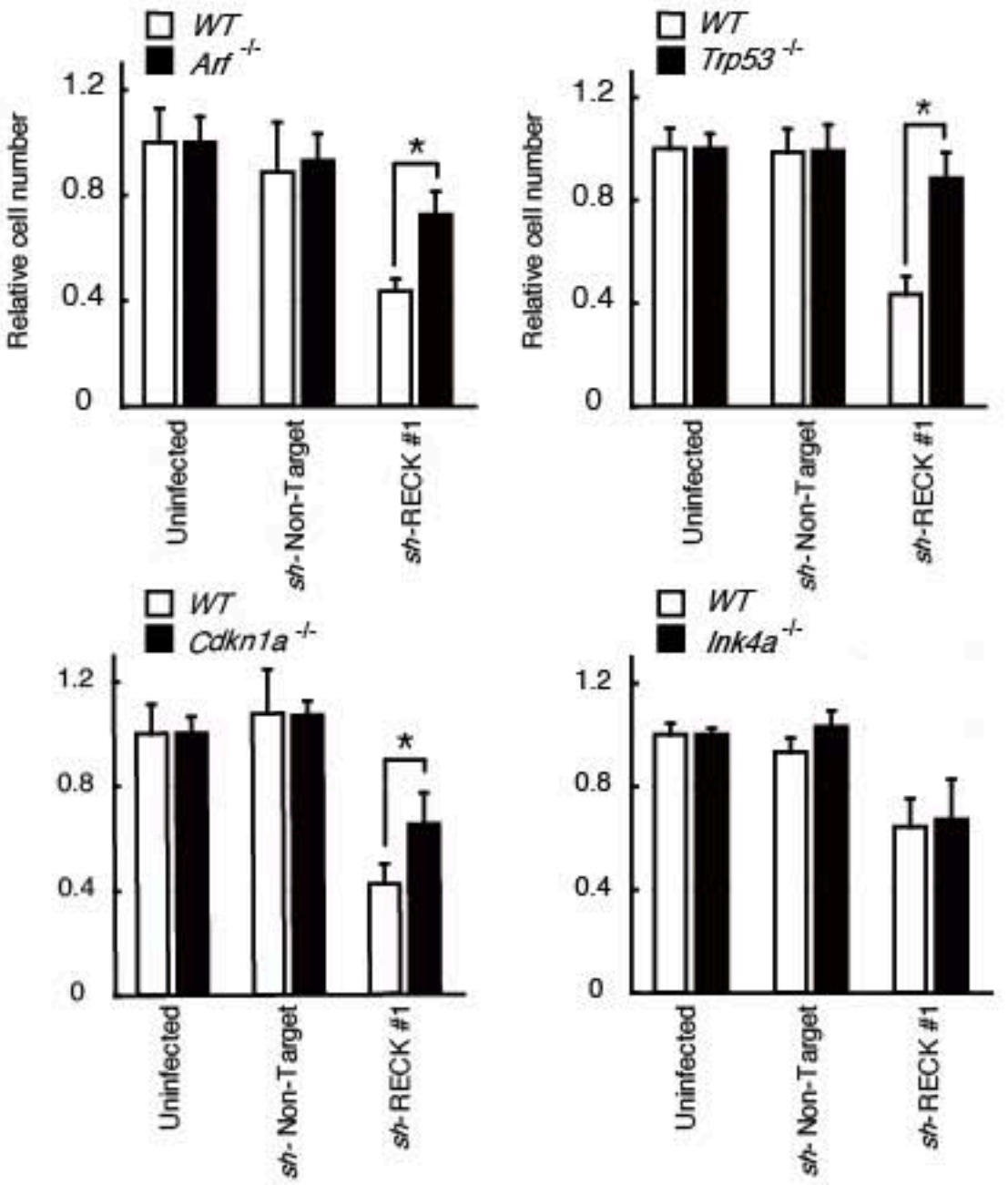

b

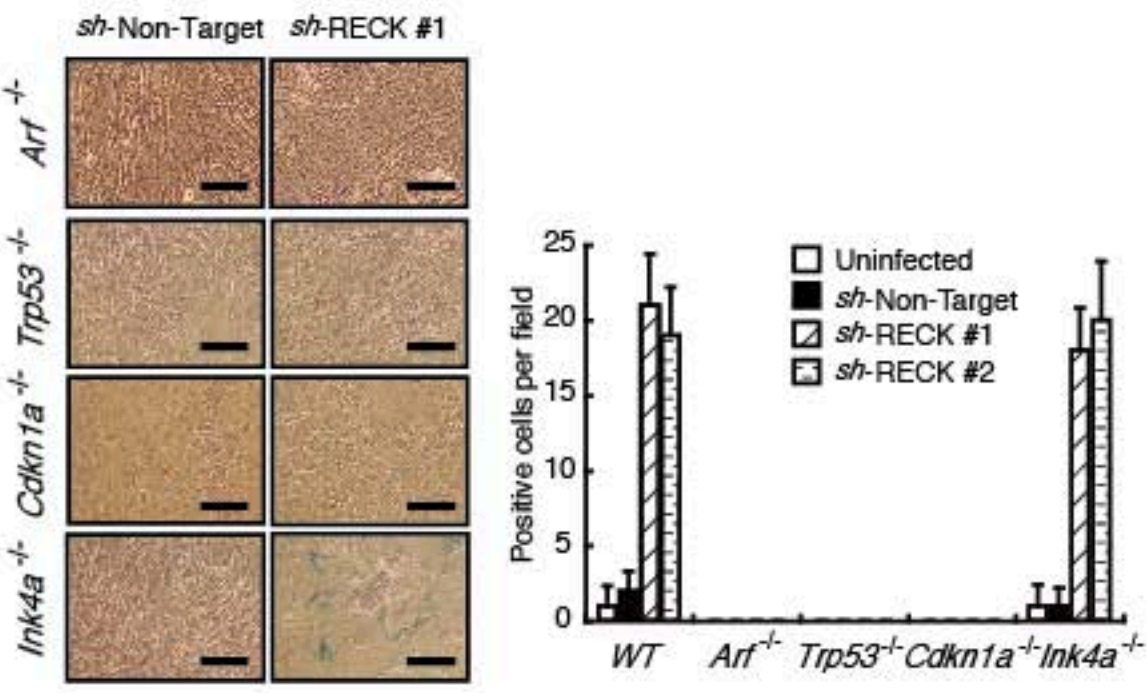

c

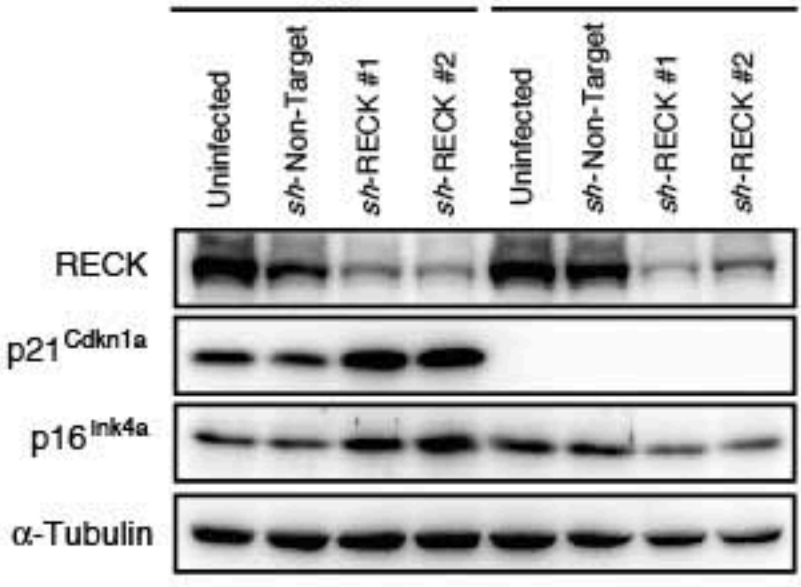

Kitajima et al., Figure 3

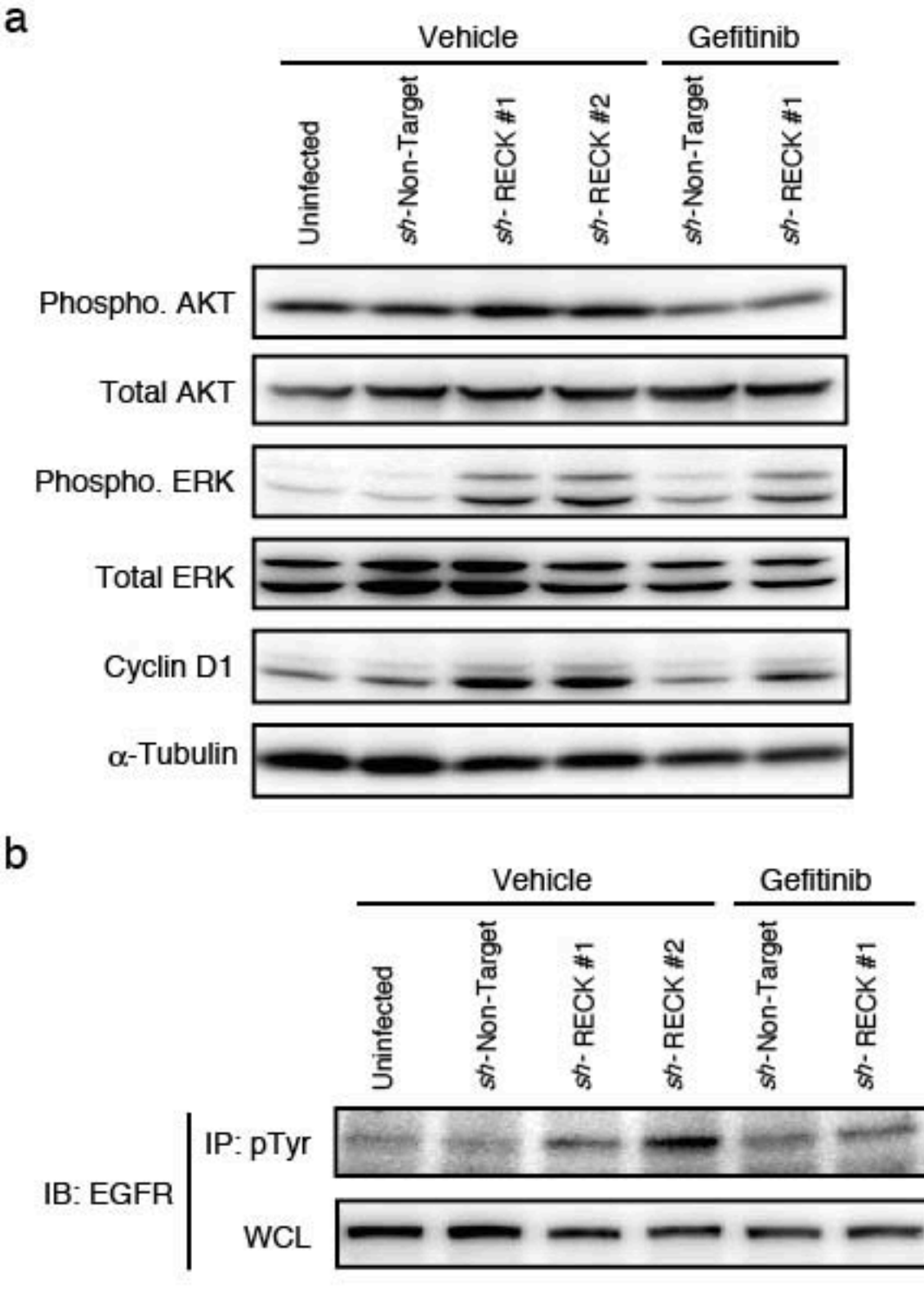

Kitajima et al., Figure 4

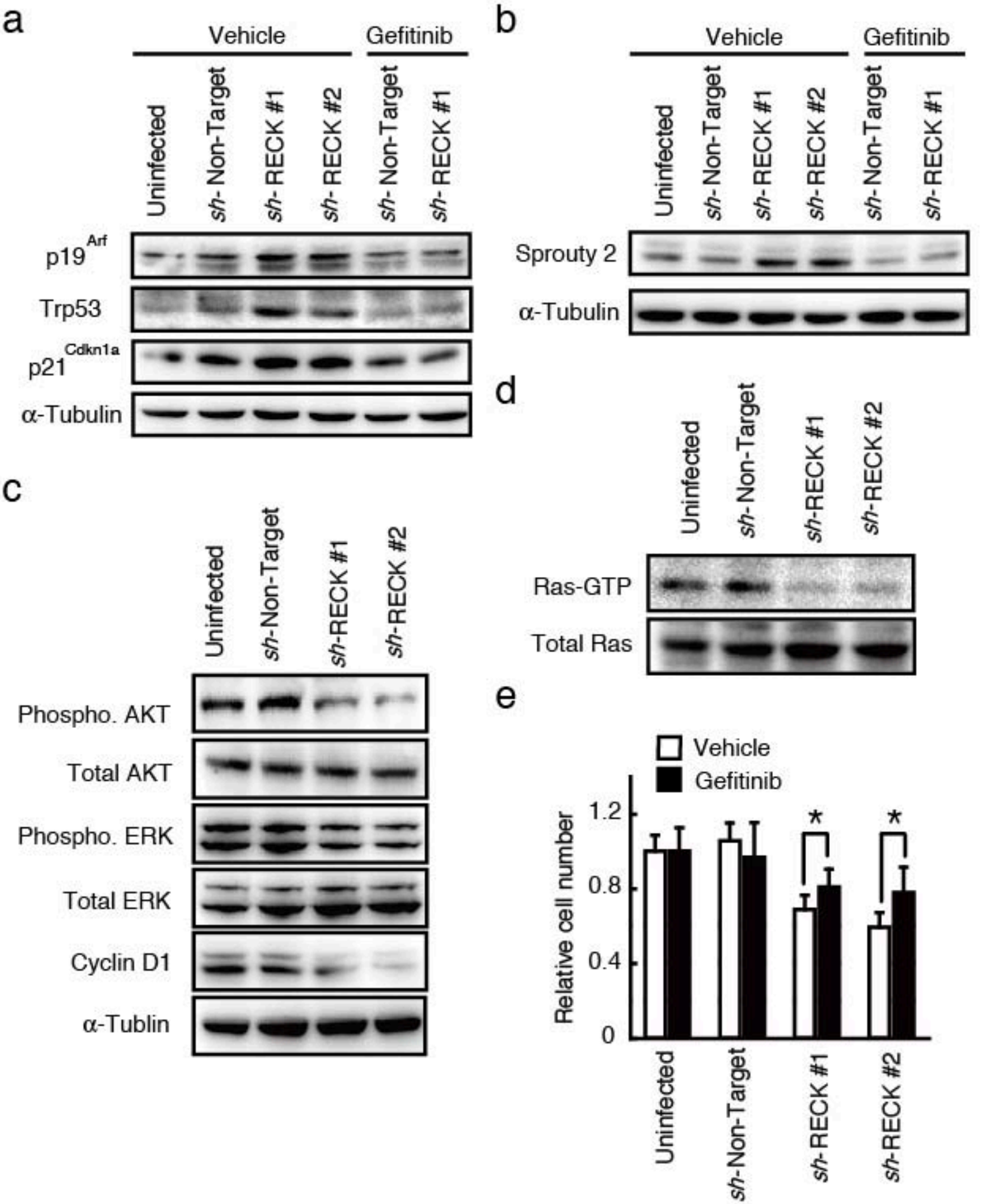

Kitajima et al., Figure 5

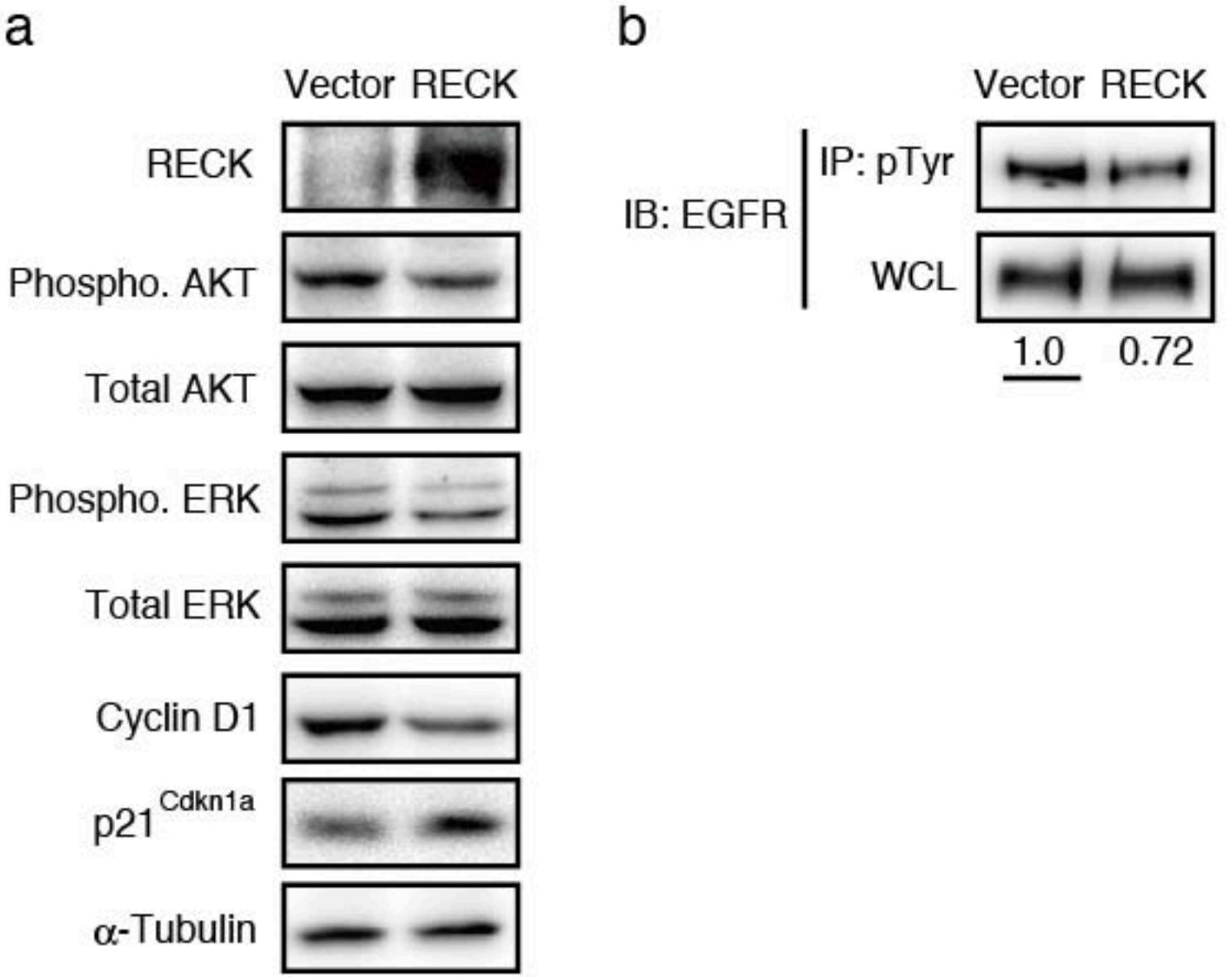

Kitajima et al., Figure 6

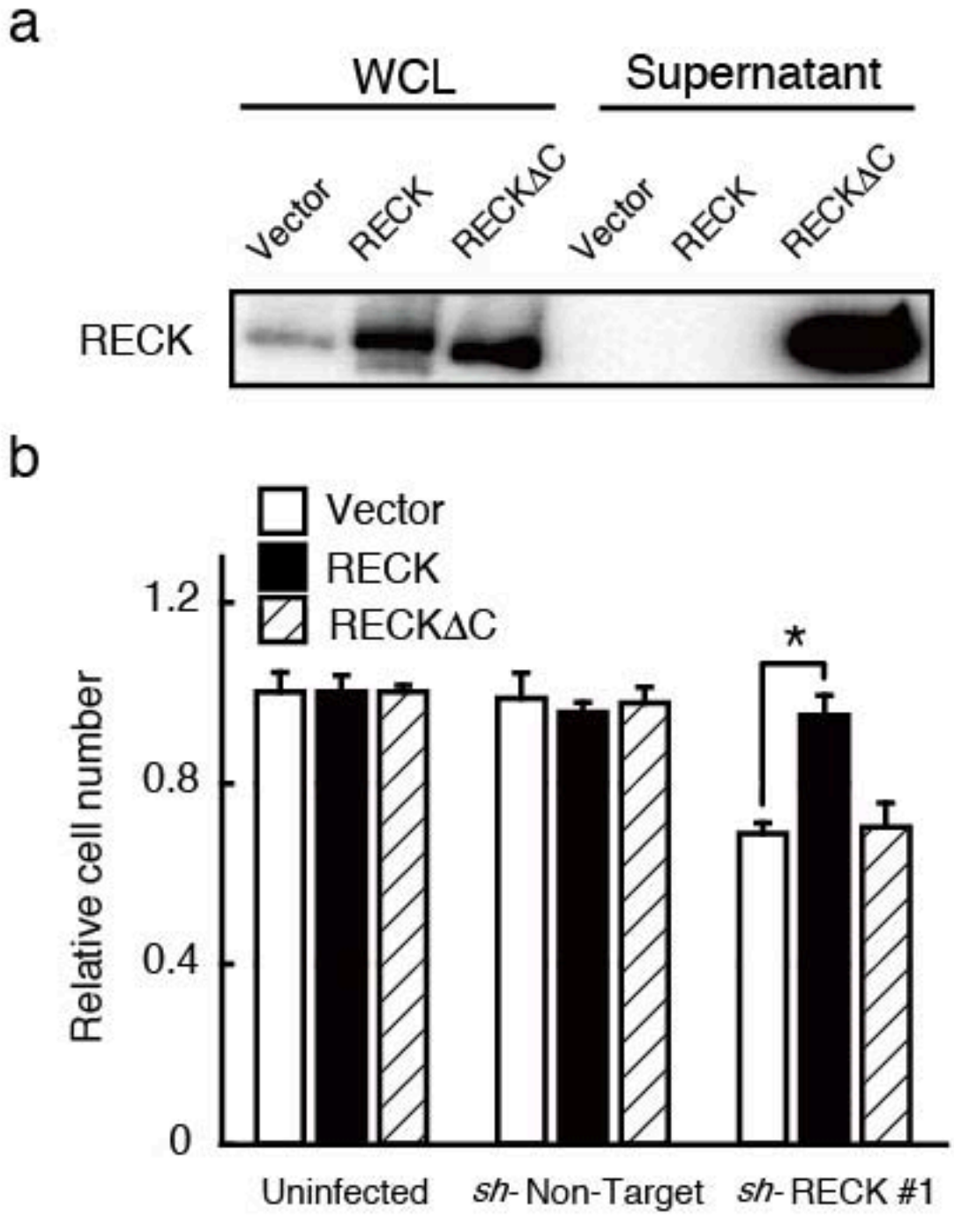

Kitajima et al., Figure 7

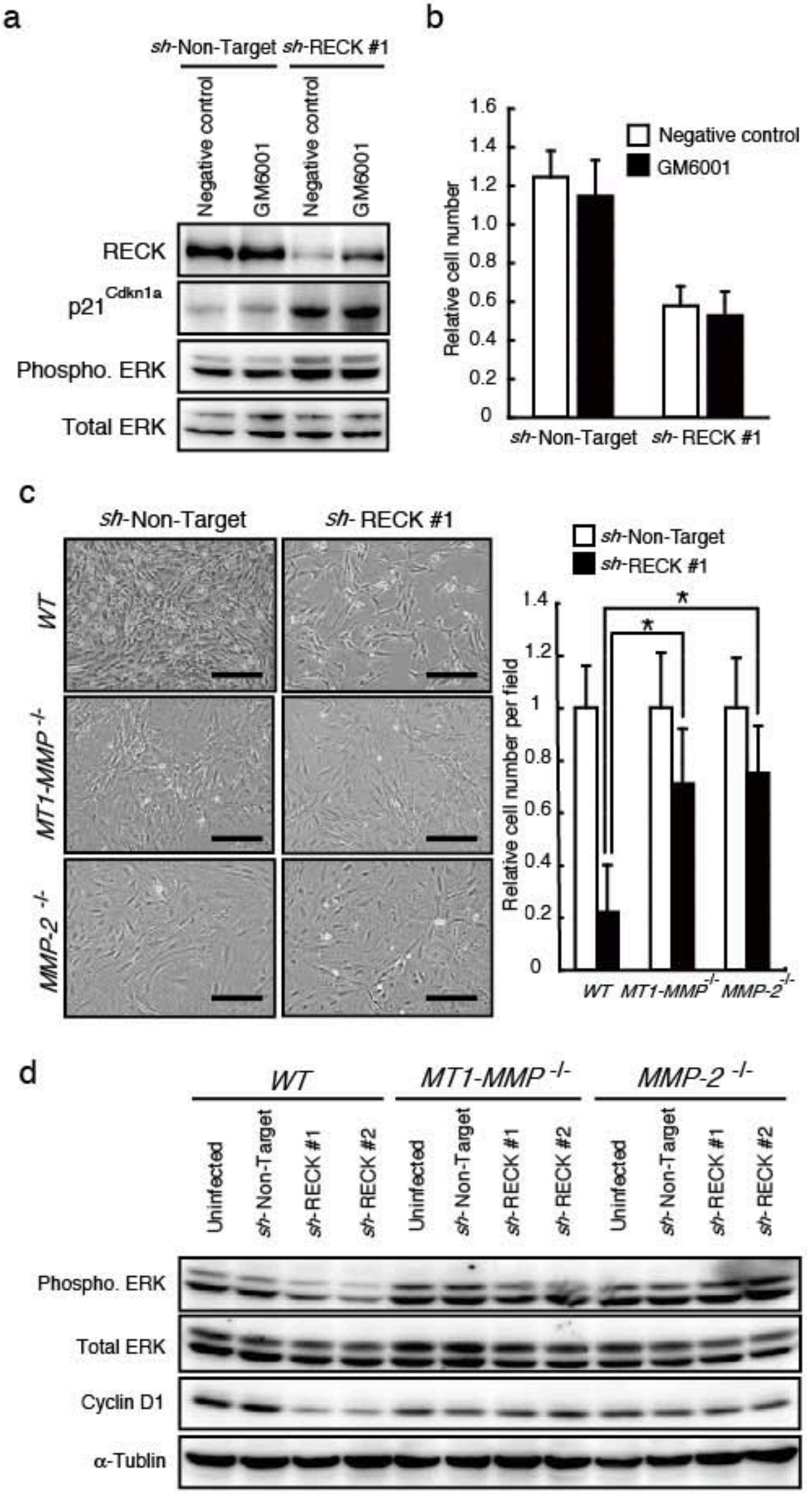

SUPPLEMENTAL DATA

Reversion-inducing cysteine-rich protein with Kazal motifs (RECK) interferes with epidermal growth factor receptor (EGFR) signaling

Running title: RECK antagonizes RAS signaling

S Kitajima[1,2], T Miki[2,3,4], Y Takegami[2], Y Kido[1], M Noda[2], E Hara[5], A Shamma[1,2,3] and C Takahashi[1,2,3]

[1]*Division of Oncology and Molecular Biology, Cancer and Stem Cell Research Program, Cancer Research Institute, Kanazawa University, Kakuma-machi, Kanazawa, Ishikawa 920-1192, Japan*
[2] *Department of Molecular Oncology, Kyoto University Graduate School of Medicine, Yoshida-Konoe-cho, Sakyo-ku, Kyoto 606-8501, Japan*
[3] *The 21st Century Center of Excellence Program, Kyoto University Graduate School of Medicine, Yoshida-Konoe-cho, Sakyo-ku, Kyoto 606-8501, Japan*
[4] *Department of Biochemistry and Molecular Biology, University of Texas Health Science Center-Houston, Houston, Texas 77030, USA*
[5] *Division of Cancer Biology, The Cancer Institute, Japanese Foundation for Cancer Research, 3-8-31 Ariake, Koto-ku, Tokyo 135-8550, Japan*

Correspondence: Professor C Takahashi, Division of Oncology and Molecular Biology, Cancer and Stem Cell Research Program, Cancer Research Institute, Kanazawa University, Kakuma-machi, Kanazawa, Ishikawa 920-1192, Japan.
E-mail: chtakaha@staff.kanazawa-u.ac.jp

Supplemental Materials and Methods

Induction of adipogenesis

An adipogenic fibroblast cell line PA6 was obtained from RIKEN BRC (RCB1127).

The cells were maintained in α-modified Eagle's medium (αMEM) supplemented with 10% fetal bovine serum (FBS), plated at a density of $1x10^4/cm^2$, and allowed to differentiate for 7 days in an differentiation-inducing medium containing 0.25 μM dexthametasone, 0.5 mM 3-isobutyl-1-methylxanthine (IBMX), and 10 μg/ml insulin.

Oil Red O staining

Cells were fixed with 4% paraformaldehyde (PFA) in phosphate-buffered saline (PBS) for 30 min, rinsed with PBS and then by 60 % isopropanol, stained with 30 mg/ml Oil Red O (Sigma) in 60% isopropanol, and again rinsed with PBS.

Antibody and reagent

Immunoblotting was performed using the following antibodies: $p27^{CDKN1B}$ (sc-528, Santa Cruz Biotechnology), PPARγ (sc-7273, Santa Cruz Biotechnology), and C/EBPα (sc-61, Santa Cruz Biotechnology).

Cell culture

The human umbilical vein endothelial cells (HUVECs: CC2517, CAMBREX) were maintained in EGM-2 bullet kit (CC-3162, CAMBREX). HUVECs were used for each experiment before 5 passages.

RNA interference

The siRNAs specifically targeting human RECK (*si*-RECK #1: 29149, *si*-RECK #2: 29155) and negative control (4611G) were purchased from Ambion, and those targeting human MMP-2 (1178208) were purchased from Invitrogen. 5 x 10^4 HUVECs were transfected with 50 mM siRNAs using Lipofectamine2000 (Invitrogen).

Legends for supplemental figures

Figure S1 RECK expression in MEFs upon serum starvation, release from starvation and contact inhibition.

(a) MEFs were incubated in αMEM containing 0.1% fetal bovine serum (FBS) for 3 days, and exposed to 10 % FBS for the indicated period of time. The expression of the indicated proteins was analyzed by IB at the indicated time point.

(b) MEFs were plated at 0.3 x 10^5 (low density), 1 x 10^5 (subconfluent) or 2 x 10^5 (confluent) (cells per 6 well-type plate), and collected after incubation for 24 h. The expression of the indicated proteins in resultant cells was analyzed by IB.

Figure S2 Impact of *RECK-Cdkn1a* double knockout on cell proliferation.
MEFs of the indicated genotype were analyzed using the 3T3 protocol.

Figure S3 Effects of acute RECK depletion on differentiation of the adipogenic fibroblast cell line PA6.
(a-b) Close-to-confluent (2 x 10^5 cells per 6 well-type plate) PA6 cells lentivirally transduced with the indicated shRNAs were cultured in growth medium for 24 h, after which cells were incubated in differentiation-inducing medium for 7 days. The resultant cells were stained with Oil Red O and photographed under light microscopy (a). The expression of the indicated proteins in cells treated as indicated was analyzed by IB (b).

Figure S4 Effects of shRNA-mediated RECK depletion on EGFR signaling in MEFs.
(a) IB of the indicated proteins in wild type MEFs transduced with the indicated shRNAs and cultured for 48 h in the presence of 0.1 % dimethyl sulfoxide (DMSO) (vehicle) or 10 μM genistein (345834, Calbiochem).
(b) Immunoprecipitation from whole lysates of cells from panel (a) with an anti-phosphorylated Tyrosine (pTry) antibody. Precipitates from 500 μg protein in whole cell lysates (upper) or 20 μg protein in whole cell lysates (lower) were analyzed by IB with anti-EGFR antibody.

Figure S5 Negative feedback to RAS signaling induced by acute RECK depletion.
(a, b) IB of the indicated proteins in wild type MEFs transduced with the indicated shRNAs for and cultured for 48 h in the presence of 0.1 % DMSO (vehicle) or 10 μM genistein.
(c) Relative numbers of MEFs at 5 days after transduction with the indicated shRNAs and treatment with 0.1 % DMSO (vehicle) or 10 μM genistein were quantified. Bars are means + SEM (n = 3). *P < 0.01 by Student's *t*-test.

Figure S6 Effects of EGF and FGF on RECK expression in MEFs.

(a) MEFs treated with 10 ng/ml EGF or 10 ng/ml FGF for 24 h in the presence of 10 % FBS were analyzed by IB for the indicated proteins.

(b) A model of the genetic interaction of RECK and RAS signaling.

Figure S7 MMP-2 dependent effects of RECK depletion in HUVECs.

(a) IB of the indicated proteins in whole cell lysates from HUVECs transfected with the indicated siRNAs and cultured for 3 days. Figure

(b) Cell proliferation of HUVECs transfected with the indicated siRNAs. Cells were plated at 5 x 10^4 cells per 6 well-type plate, cultured for 48 h, and photographed under light microscopy (left). The cell number of HUVECs transfected with the indicated siRNAs was quantified (right). Scale bar: 500 μm. Bars are means + SEM (n = 4 fields). *P < 0.01 by Student's *t*-test.

Kitajima et al., Figure S1

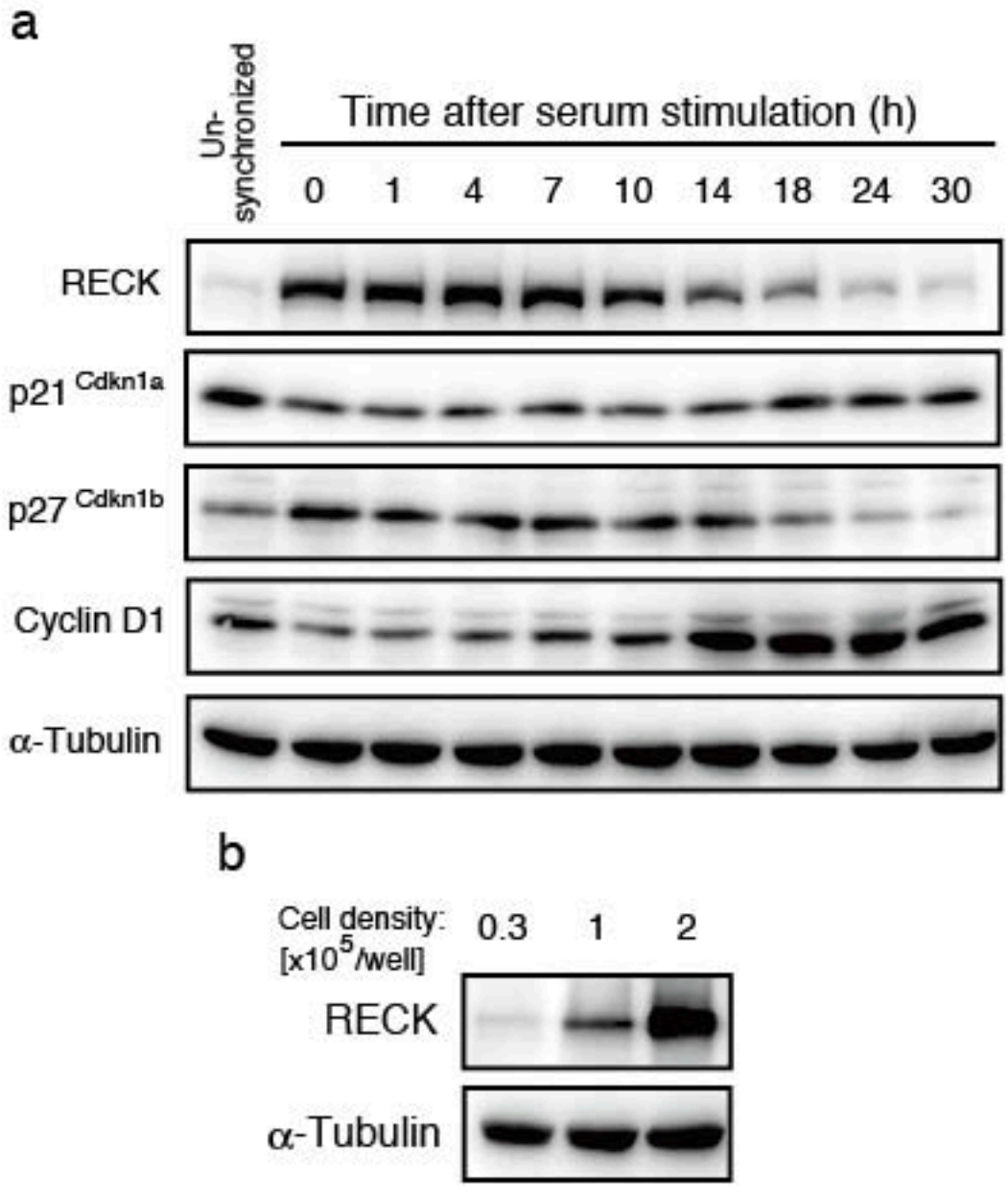

Kitajima et al., Figure S2

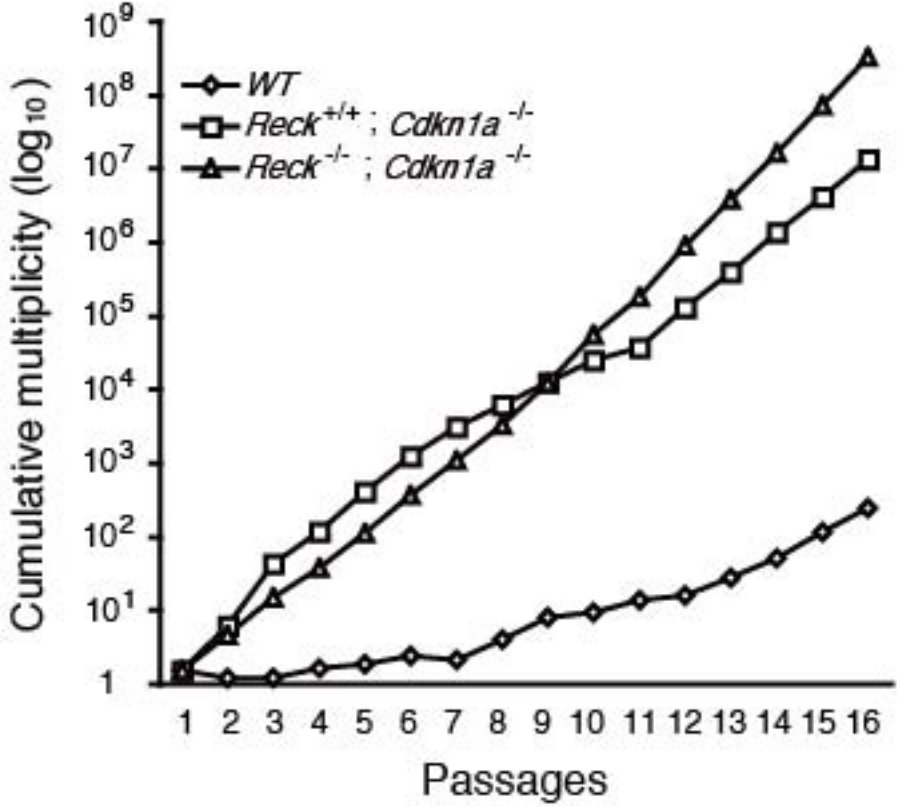

Kitajima et al., Figure S3

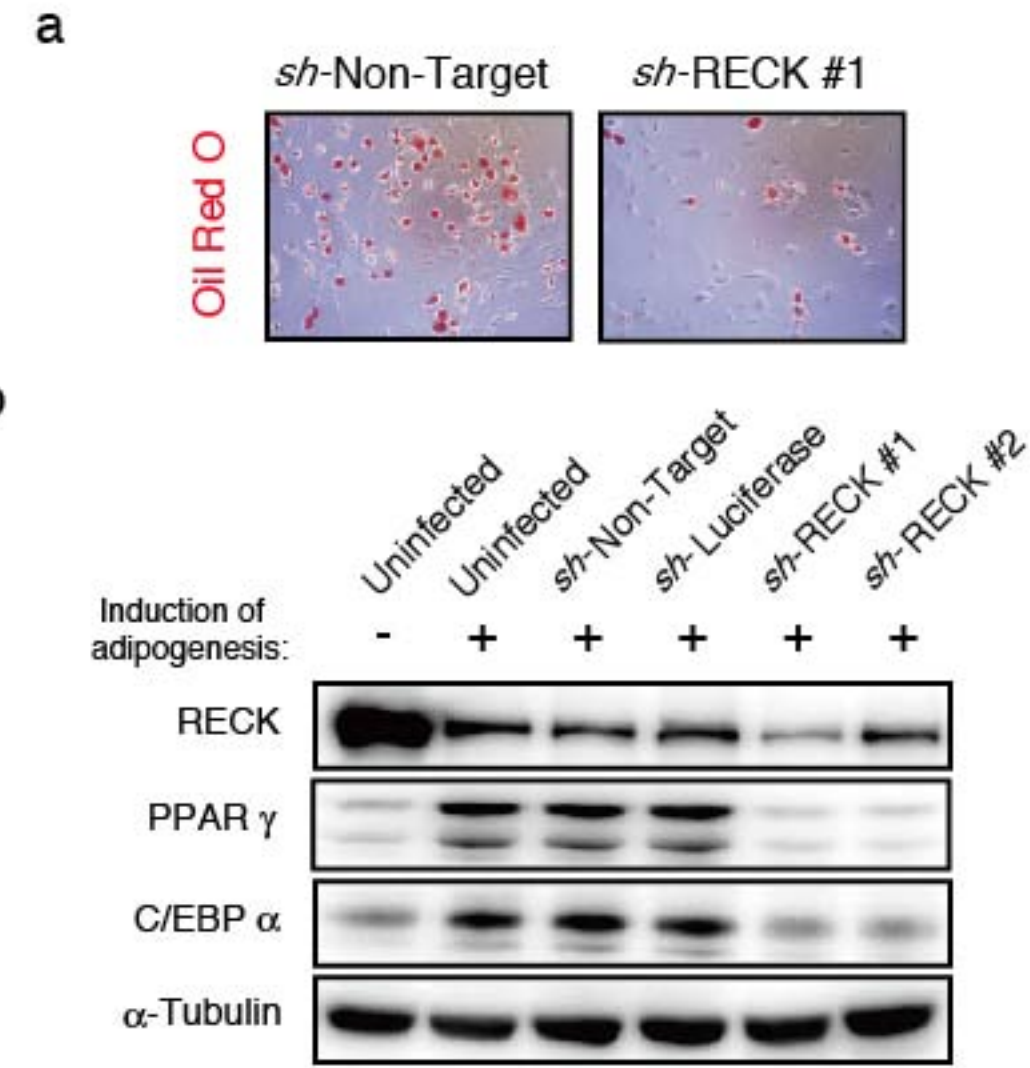

Kitajima et al., Figure S4

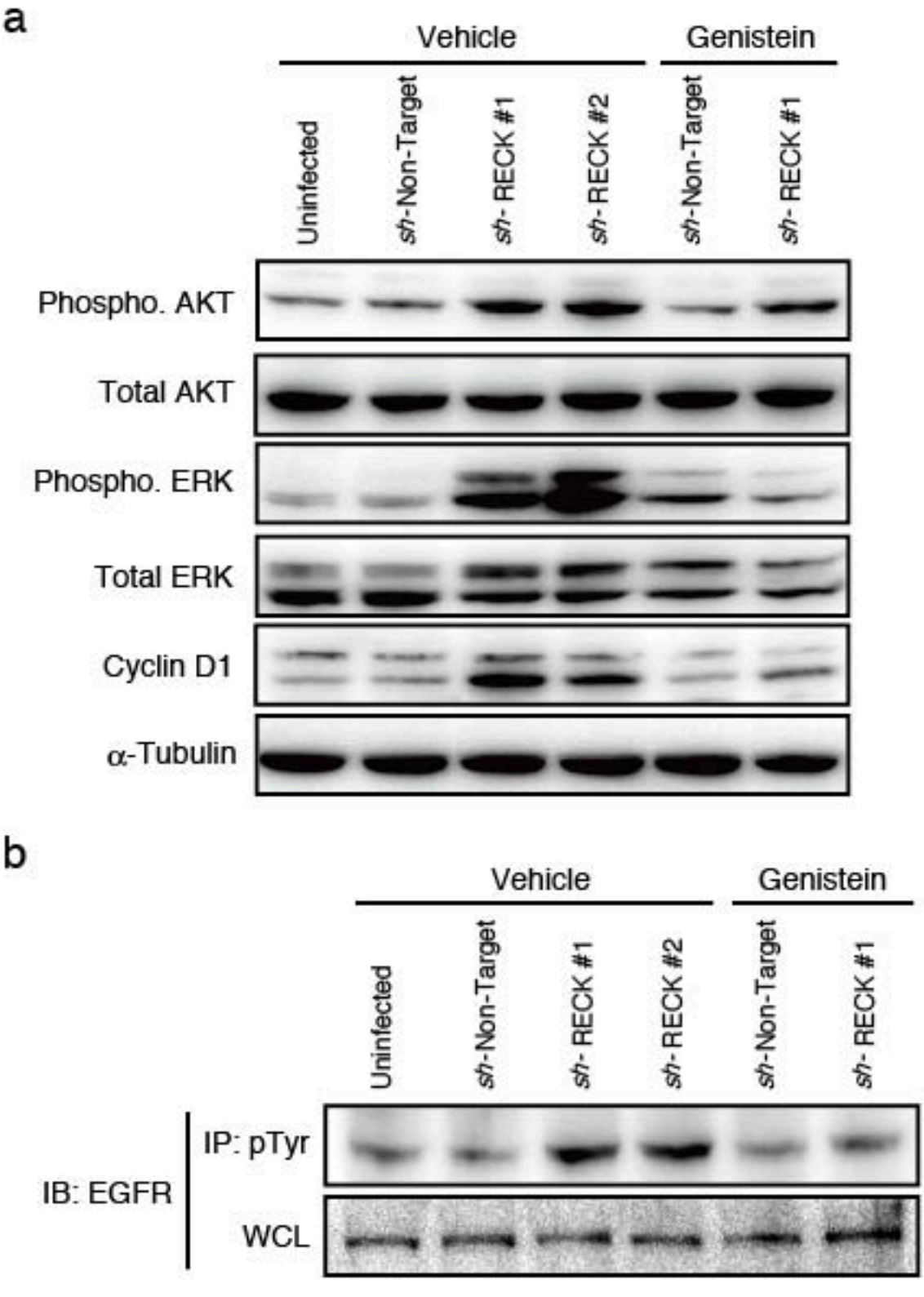

Kitajima et al., Figure S5

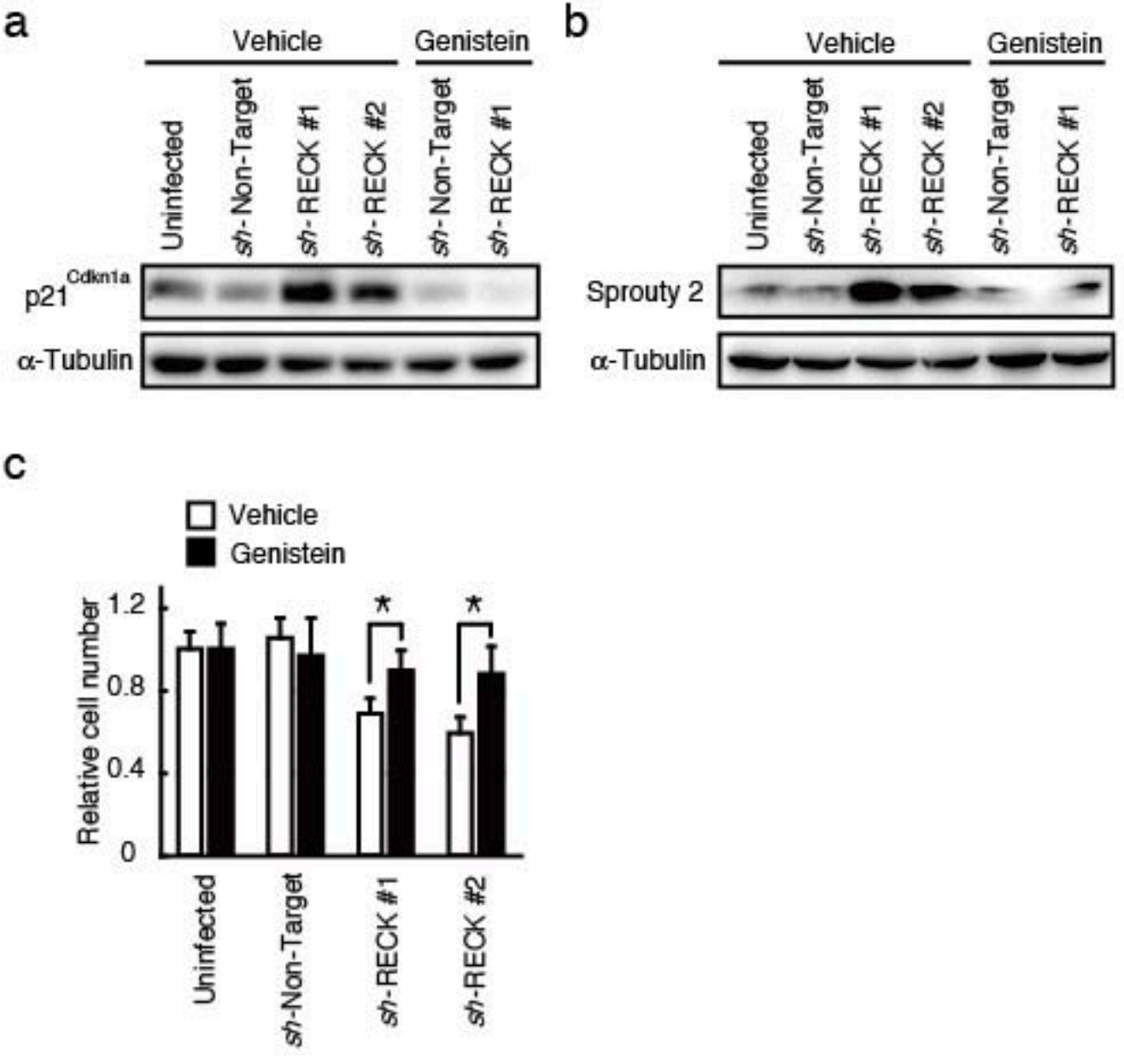

Kitajima et al., Figure S6

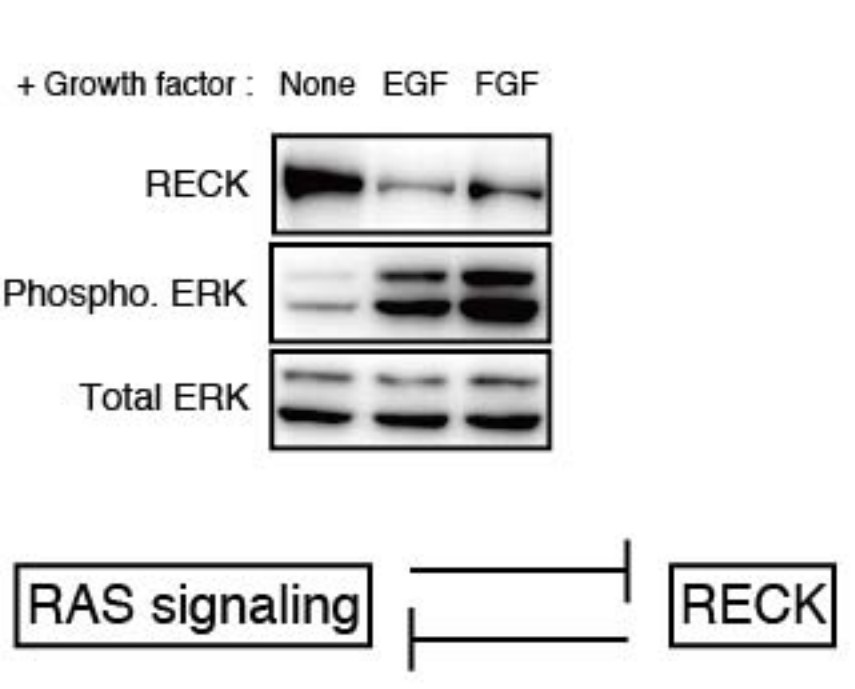

Kitajima et al., Figure S7

a

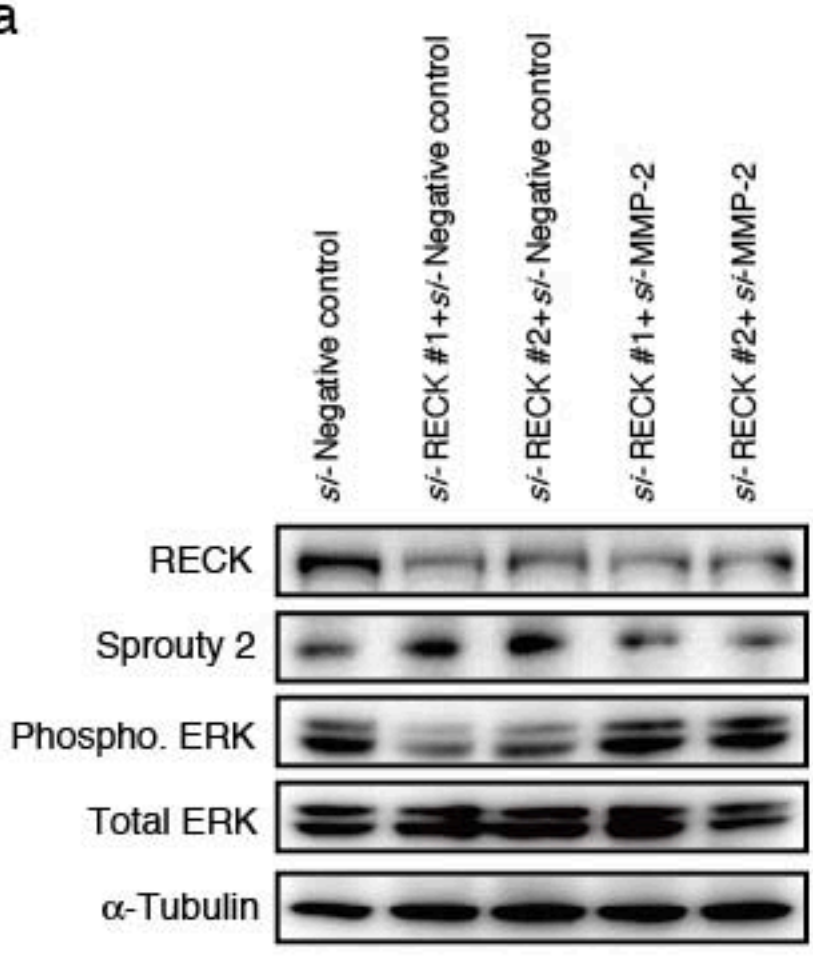

b